Responses to Editor:

Both reviewers raised major concerns with this manuscript, which I don't think have been sufficiently addressed in either the response or the revisions. I share the reviewers' concerns about the experiment design used in this study, and would like to see these addressed in more detail before returning the manuscript to the reviewers.

Thank you for your comments. We appreciate your feedback. We have carefully revised the manuscript and addressed these concerns in detail. Please find our point-by-point responses below (in blue).

The observed precipitation trend is evaluated based on only 10 years of data, and there is no discussion of how this trend compares to either longer term trends, or internal variability. The trend is also based on only one observational dataset.

• I think it is important that we see a comparison between the GPM data and other precipitation datasets such as GPCP to give a sense of how robust this observed trend is.

We acknowledge the concern regarding the reliance on a single observational dataset for evaluating precipitation trends. To address this, we have compared the GPM dataset with ERA5 and GPCP precipitation data (Fig. S14). Our analysis shows that all three datasets exhibit a similar decreasing trend in precipitation over Australia, reinforcing the robustness of the observed trend. We have incorporated this comparison into the revised manuscript (Results section): "The GPM and GPCP data also exhibit a similar decreasing trend in precipitation over Australia, reinforcing the robustness of the observed drying trend (Figure S14)."
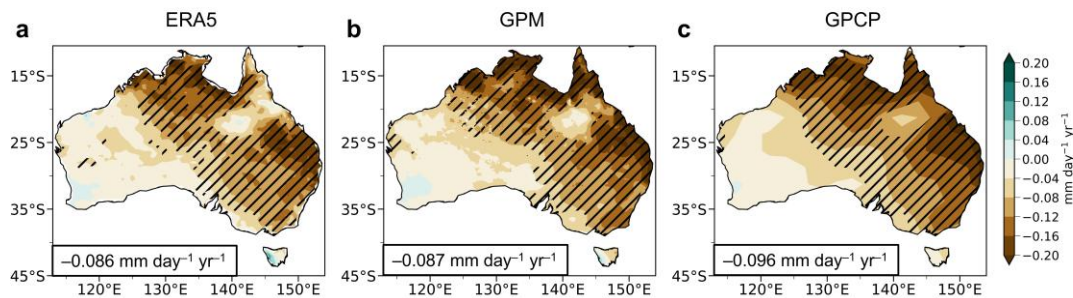

Figure S14. Linear trends of observed precipitation rate in Australia based on ERA5, GPM, and GPCP. Spatial distributions of linear trends annual mean precipitation rate (unit: mm day^{-1}) in Australia during 2010–2019 from ERA5 (a), GPM (b), and GPCP (c) datasets. The shaded areas indicate trends are statistically significant at the 90% confidence level. Regional averages over Australia are noted at the bottom-left corner of panels.

• It is also important that the authors show a longer precipitation timeseries, and evaluate the interannual variability, to give some context to the magnitude and significance of the trend. Reviewer 2 is concerned that 2010 and 2011 were anomalously wet, and thus bias the trend. They have plotted data from 2000 – I ask the authors to at least do the same, and would strongly encourage them to plot an even longer timeseries to provide more context. It is stated in the abstract that Australia experienced anomalously dry and warm conditions since the 2010s, but, beyond a few citations, there isn't any evidence in the manuscript to support this.

34 Thank you for your suggestion. As per your request, we have extended the time series of
35 precipitation covering 2001–2019 in Fig. S12. The updated figure clearly shows an increasing
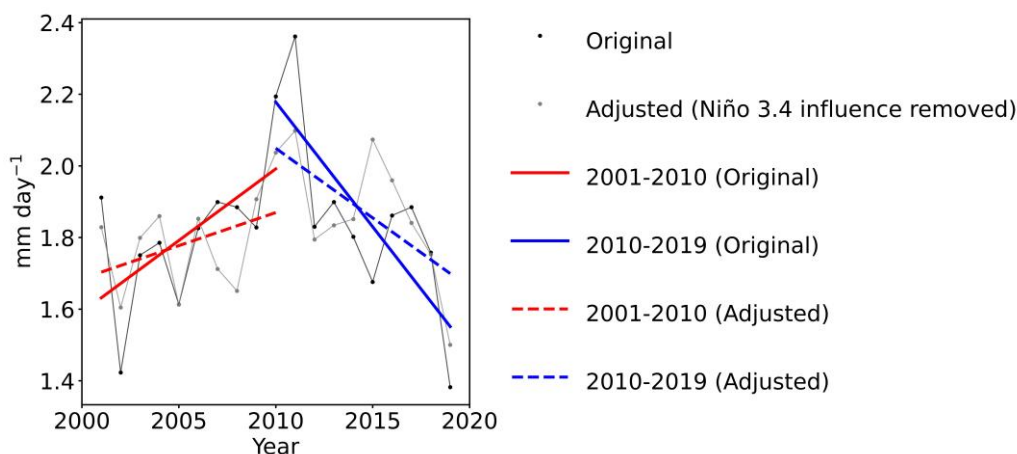36 precipitation trend during 2001–2010, followed by a decreasing trend during 2010–2019.

37

Figure S12. Linear trends of observed precipitation rate during 2001–2019 based on ERA5.
39 The time series of annual mean precipitation rate (unit: mm day^{-1}) over Australia during 2001–
40 2019 from ERA5 reanalysis. The linear trends for the periods 2001–2010 and 2010–2019 are
41 indicated. The time series are also given after removing the influence of Niño 3.4 index.
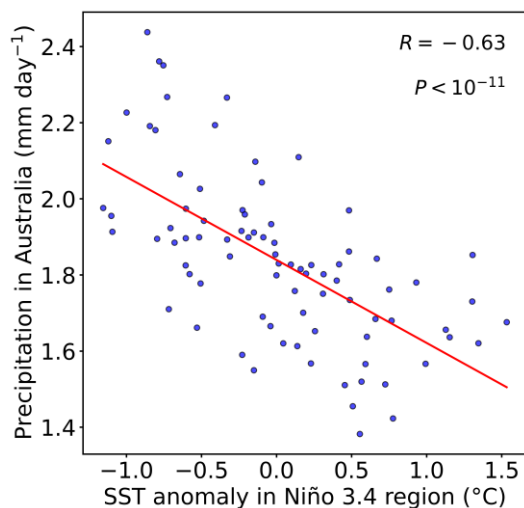

42

Figure S13. Scatter plot showing the correlation between SST anomaly in Niño 3.4 region
44 **and precipitation in Australia.** The red line represents the linear regression fit to the data, with
45 the corresponding correlation coefficient (R) and p-value displayed in the figure.

46 • In the response document, the authors state that the observed trend is calculated from 2010-2019
47 instead of 2013-2019 to minimize the internal variability. This is still a very short time period, and
48 a quantitative assessment of internal variability is required if readers are to be confident that it is a
49 forced trend.

50 To account for the potential influence of internal variability, particularly ENSO, which is a major
51 driver of Australia's precipitation variability (Fig. S13), we have also adjusted the precipitation
52 data by removing the influence of Niño 3.4 index. The adjusted results exhibit a similar transition,

53　confirming the robustness of the observed forced drying trend since the 2010s (Fig. S12).

54　The reviewers also raise important concerns about the experiment design, which warrant more
55　discussion than they have been given in the current response and revision. I am not convinced by
56　the response to reviewer 2, and think the authors undermine their own interpretation of their results
57　in this response. Equilibrium runs are an excellent tool for understanding the physical response to
58　forcing, and for identifying the mechanisms for particular responses, as the authors have done in
59　this study. However, care needs to be taken when comparing them to real-world changes. As the
60　authors state in their response, 'the relatively short period from 2013 to the present may not provide
61　enough time for the climate system to fully respond to aerosol changes'. But, this full response is
62　exactly what their equilibrium simulations show. So, how can these experiments be used to
63　quantify an aerosol contribution to an observed trend, as the authors do in their manuscript? Is it
64　possible to use such simulations to make anything more than qualitative statements about observed
65　trends? One could perhaps quantify the Chinese aerosol contribution to a modelled response, but
66　this would require other forcings to be considered. Reviewer 2 is recommending rejection of the
67　manuscript based on the experiment design. I would like to see a more detailed discussion of the
68　design of the study, and the implications of comparing several hundred years of simulated
69　equilibrium responses to just 10 years of observed data, in both the response to the reviewers and
70　the revised manuscript before making a decision.

71　Thank you for your insightful comments regarding the experiment design and the comparison
72　between equilibrium simulations and observed trends. We acknowledge the limitations of our
73　approach and have carefully revised the manuscript accordingly. The equilibrium simulations
74　primarily capture the long-term climate response to aerosol forcing, whereas the observed trends
75　over a decade are influenced by both forced responses and internal variability. While our
76　simulations provide valuable insights into the physical mechanisms linking aerosol reductions to
77　climate changes, they are not intended for direct quantitative attribution of observed trends. **To
78　clarify it, we have removed all statements that directly attribute the observed trend to the
79　simulated aerosol response in a quantitative manner and now emphasize that the simulations
80　serve as a tool for understanding the underlying processes rather than quantitatively
81　estimating real-world aerosol-induced changes.** Moving forward, we recognize that transient
82　simulations would be better suited for capturing short-term forced trends, and we plan to
83　incorporate them in future studies to further investigate the evolution of short-term responses and
84　assess the potential contributions of other external forcings, such as greenhouse gases and internal
85　variability.

86　I am confused by the interpretation of the low bias in the PM2.5 and AOD trends in CESM1 found
87　in the response and the revised manuscript. CESM1 is known to underestimate PM2.5. The authors
88　have calculated a change in PM2.5 and found that it is small compared to the observed change. If
89　this is based on an absolute change, and the background PM2.5 in the model is low, then one would
90　also expect the change to be small compared to observations. However, even though aerosol
91　concentrations and AOD in the model are low, CESM1 has a relatively large aerosol forcing. Thus,
92　a small absolute change in PM2.5 or AOD may result in a large forcing in the model. I don't think
93　a small absolute change in the model necessarily implies an underestimate of the forced response.
94　How do the percentage changes in PM2.5 and AOD in the model compare to the percentage
95　changes in observations, for example?

96　Thank you for your valuable comment. We acknowledge the known low bias in $PM_{2.5}$ and AOD
97　in CESM1 and appreciate the need for a more nuanced interpretation of the model's response. In

our original analysis, we primarily compared absolute changes, which may not fully capture the model's sensitivity to aerosol forcing given its relatively strong aerosol-cloud interactions. To address this, we have now included a comparison of percentage changes in PM$_{2.5}$ and AOD between the model and observations (Fig. S4 and Fig. S5). This allows for a more direct assessment of whether the model underestimates the forced response, independent of its background aerosol concentrations. We do note that the underestimation of relative concentrations is much smaller. The revised discussion clarifies that although CESM1 underestimates aerosol concentrations, the strong climate sensitivity of the model to aerosol forcing suggests that the simulated climate response may not be significantly underestimated.
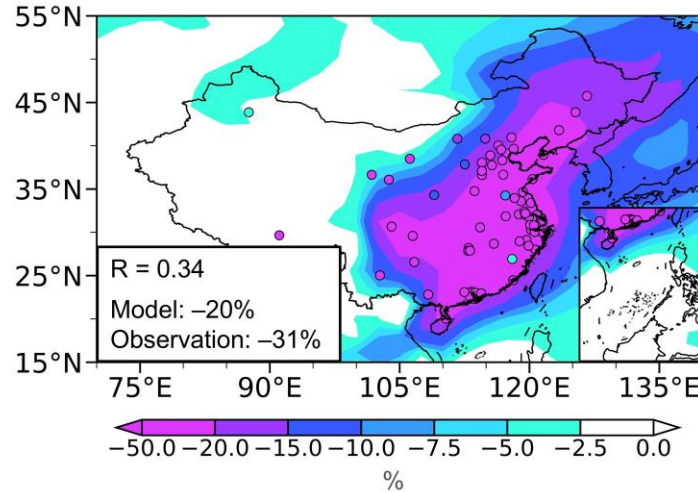

Figure S4. Comparisons of relative changes in near-surface PM$_{2.5}$ concentrations between observation and model simulation. Spatial distributions of observed (circles) and modeled (shades) annual mean relative changes (2017–2019 minus 2013–2015, relative to 2013–2015) in near-surface PM$_{2.5}$ concentration (unit: %). Relative changes of observation and model simulation and correlation coefficient (R) between observation and simulation are shown at the bottom-left corner of the panel.
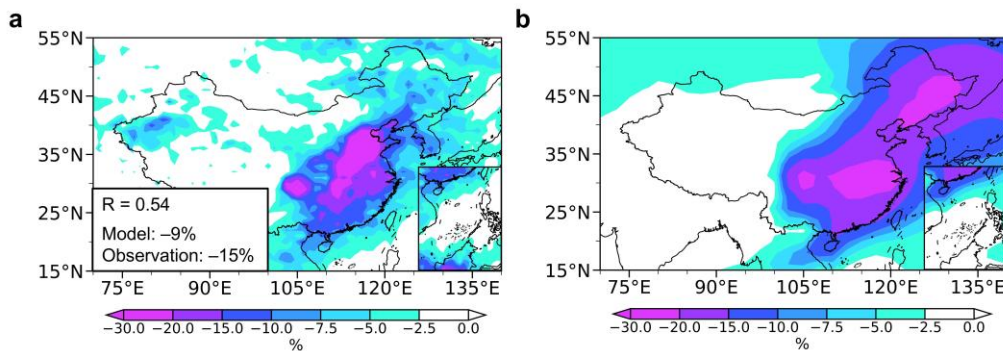

Figure S5. Comparisons of relative changes in aerosol optical depth (AOD) between satellite retrieval and model simulation. Spatial distributions of annual mean relative changes (2017–2019 minus 2013–2015, relative to 2013–2015) in Moderate Resolution Imaging Spectroradiometer (MODIS) (**a**) and modeled (**b**) AOD (unit: %). Relative changes of observation and model simulation and correlation coefficient (R) between observation and simulation are shown at the bottom-left corner of panel a.

121 Thinking back to the discussion of precipitation, it would also be good to know more about the
122 significance of the observed trend. The emission reductions have been very large, but how
123 significant is the change in AOD? Is there potentially a contribution from internal variability here
124 that accounts for some of the model underestimate of the change relative to observations?

125 Thank you for your thoughtful comment. The observed AOD trend can indeed be affected by
126 factors beyond anthropogenic aerosol changes, such as meteorological variability and natural
127 aerosol sources. However, Zhai et al. (2019) estimated that only 12% of the $PM_{2.5}$ decrease in
128 China during 2013–2018 was attributable to meteorology. Given the substantial magnitude of
129 emission reductions, the influence of these other factors is relatively minor, and the observed AOD
130 trend remains statistically significant over large regions of China (Fig. R1). This significant
131 decreasing AOD trends in observations have also been reported in many previous studies.
132 Therefore, we don't think the modeled AOD bias could be largely attributed to the internal
133 variability in observations. We have revised the manuscript to clarify these points.
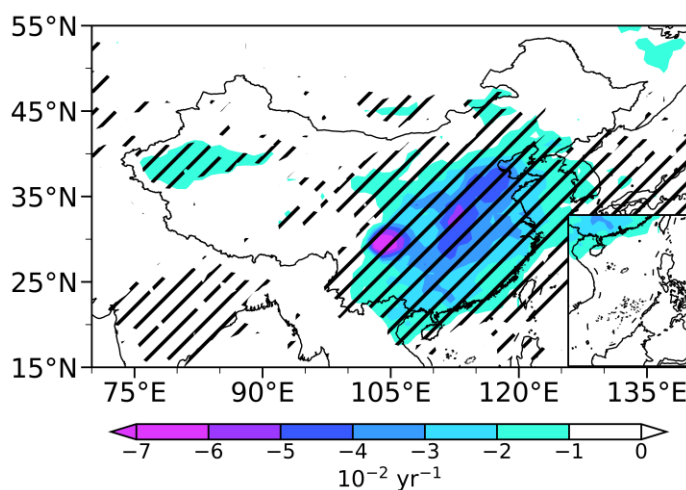

134

Figure R1. Linear trends of observed AOD in Australia based on MODIS. Spatial distributions
of linear trends of annual mean AOD (unit: unitless) in China during 2010–2019 from MODIS.
The shaded areas indicate trends are statistically significant at the 90% confidence level.

138 In addition to addressing the major comments above:

139 • it is necessary to improve the indication of significance on the map figures in the manuscript.
140 The shading is difficult to see in many of the figures, both on my screen and on a printout.

141 The indication of significance in all map figures has been modified for improved clarity.

142 • I would like to see some discussion of how these results compare to previous studies assessing
143 the Australian precipitation response to Asian aerosols. Rotstayn et al. (2007) and Fahrenbach et
144 al. (2023) are cited in the introduction, but are absent from the results and discussion sections.

145 Thank you for your suggestion. We have now incorporated a discussion comparing our findings
146 with previous studies, particularly Rotstayn et al. (2007) and Fahrenbach et al. (2023).

147 "Rotstayn et al. (2007) and Fahrenbach et al. (2023) investigated the impact of increasing
148 anthropogenic aerosols over Asia during the late 20th century and early 21st century and indicated
149 that enhanced aerosol emissions strengthened the meridional temperature and pressure gradients,
150 intensifying the monsoonal circulation and leading to increased precipitation over Australia. In

contrast, our study focuses on the recent reductions in anthropogenic aerosols in China since 2013, showing that the aerosol reductions reversed circulation changes induced by the previous aerosol increases and contributed to drying rather than increased rainfall over Australia. Our study also explores the subsequent impact of aerosol reductions in China on Australian temperature. We find that reduced moisture availability over Australia led to a shift in surface energy partitioning, with more energy being converted into sensible heat rather than latent heat, resulting in near-surface warming. In summary, while previous studies have demonstrated the role of increasing Asian aerosols in enhancing Australia's precipitation, our work complements these findings by showing that decreasing aerosols, particularly from China, can drive the opposite effect, contributing to both drying and warming conditions in Australia."

The text above has been added to the Conclusion and discussion section.

References

Zhai, S., Jacob, D. J., Wang, X., Shen, L., Li, K., Zhang, Y., Gui, K., Zhao, T., and Liao, H.: Fine particulate matter ($PM_{2.5}$) trends in China, 2013–2018: separating contributions from anthropogenic emissions and meteorology, Atmos. Chem. Phys., 19, 11031–11041, https://doi.org/10.5194/acp-19-11031-2019, 2019.

Responses to Referee #1:

This research article investigates the impact of anthropogenic aerosol reductions in China on Australia's climate. The study found that the decline in Chine's aerosols since 2013 contributed to drier and warmer conditions in Australia by altering temperature and pressure gradients, which intensified the Southern Trade Winds and caused moisture divergence over Australia. The study also links these climate changes to an increase in wildfire risks in Australia. This research highlights the significant influence of distant aerosols on regional climate and offers insights for drought and wildfire risk mitigation.

The manuscript is interesting, well written and tackles an important topic of research (i.e., impact of Chinese aerosols on Australian climate). However, some technical details between the comparison of modelling results and observations need to be corrected and the selection of figures should be adjusted. I recommend acceptance of the manuscript if the major comment below can be addressed.

We thank the reviewer for the constructive suggestions, which are very helpful for improving the clarity and reliability of the manuscript. Please see our point-by-point responses (in blue) to your comments below.

Major comments

One of my main comments is related to the comparison of observation/reanalysis data and simulated results: There seems to be some inconsistency between the timeperiods used. In the method section it is mentioned that the period 2013-2019 is used for the observation/reanalysis data as well as the simulated data. However, in the captions of the supplementary figures as well as in the description of these figures in the text (e.g. L274, 278) it is mentioned that the observations are for 2010-2019. Please clarify if the same timeperiod is used for observation/reanalysis data and modelling data and if that is not the case, the plots have to be redone for the correct timeperiod to ensure an accurate comparison. Besides, is this warming and drying trend over Australia still continuing or why did the authors look at the time period 2013-2019?

The warming and drying trends in Australia due to the reduction of aerosols in China were simulated based on the two simulations with anthropogenic emissions of aerosols and precursors at years 2013 and 2019. It is because China implemented the "Air Pollution Prevention and Control Plan" in 2013 and established nationwide $PM_{2.5}$ observation sites in 2013. Whether the simulated climate responses can be detected in the real world requires the observational evidence. However, the seven years of period 2013–2019 are too short to fully capture the trends in climate variables, as various natural variabilities could influence temperature and rainfall in Australia. For example, climate variabilities, such as ENSO, can have significant impacts on the Australian monsoon and rainfall patterns and influence the long-term trends of temperature and precipitation in Australia. Therefore, we included more years to calculate the trends of the climate variables in observations. It will not affect the results since that the aerosol reductions in China only account a small amount of the changing climate in Australia. The trends in observations are calculated during 2010–2019 to minimize the internal variability. Regarding whether the trend is continuing, CSIRO and BOM (2022) reported that the warming is still ongoing in Australia and the drying trend is still ongoing

7

210   in Northern Australia, which could be contributed by the further reductions in Asian aerosols.

211   While it is great that the author's tried to reduce the figures in the main text to only 4 to explain
212   the whole story, in particular the mechanistic analysis (Section 3.2) is difficult to follow for the
213   reader with the limited number of figures. For instance, a combination of Figure S16 and S17 (i.e.
214   the filled contours showing the SST pattern overlaid by the climatological wind field) would be a
215   relevant figure to show. Additionally, Figure S21 is heavily referenced in the manuscript but the
216   figure is only shown in the supplementary. Besides, maybe a small schematic of the described
217   mechanism similarly as in Fahrenbach et al. 2024 would be helpful to guide the reader through the
218   description.

219   As requested, we have moved several figures in the main text and added the schematic diagram as
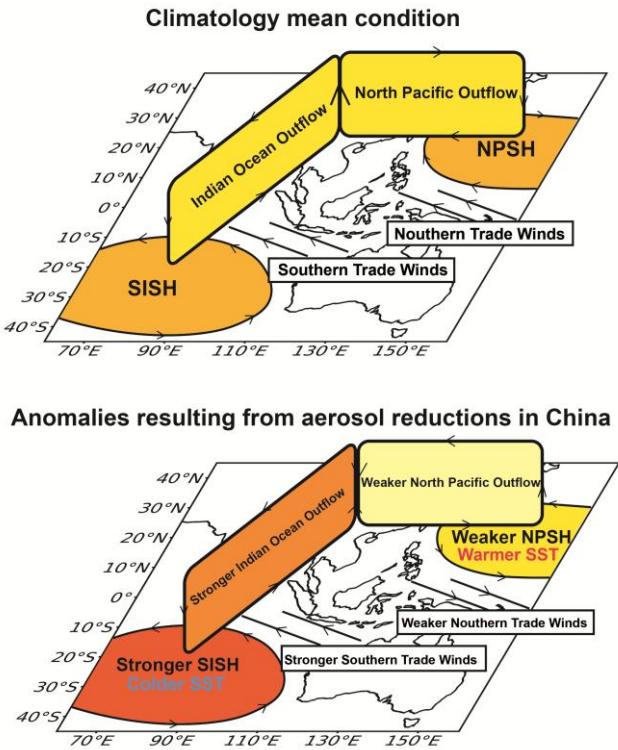220   shown below.

221

Figure 6. Schematic of the response in large-scale 3D circulations in the Asian-Pacific region to aerosol reductions in China. The top panel shows climatology mean condition, and the bottom panel shows anomalies resulting from aerosol reductions in China.

225   On the topic of figures, it would be important to show a comparison of the simulated changes with
226   the observed precipitation pattern (Figure S8) as well as the observed wind changes (Figure S18).
227   This is particularly relevant since the authors are trying to do an "attribution" study and it has to
228   be quantified that the observed and modelled changes agree. Additionally, the authors claim that
229   the modelled and observed wind changes are similar (L319-321). While I do acknowledge that 3D
230   wind changes are not the most reliable fields in reanalysis data, this is a bit of an overstatement.
231   Figure S18b and c show very few significant changes making it difficult to understand the
232   simulated flow and Figure S18d shows the largest significant trends in the winds east of Borneo

233 and around stronger southern Trade winds based on the simulated data. Maybe the authors could
234 think about showing all wind vectors and colouring the significant ones in, so that the reader can
235 at least see if the observations show the same trend even if they might not be significant based on
236 this test?

237 Thank you for your suggestion. We have revised the figure displaying the 3D wind fields, with
238 significant and insignificant circulations clearly distinguished. Although only a few significant
239 changes persist in Northern Australia, the large-scale circulations around Australia show noticeable
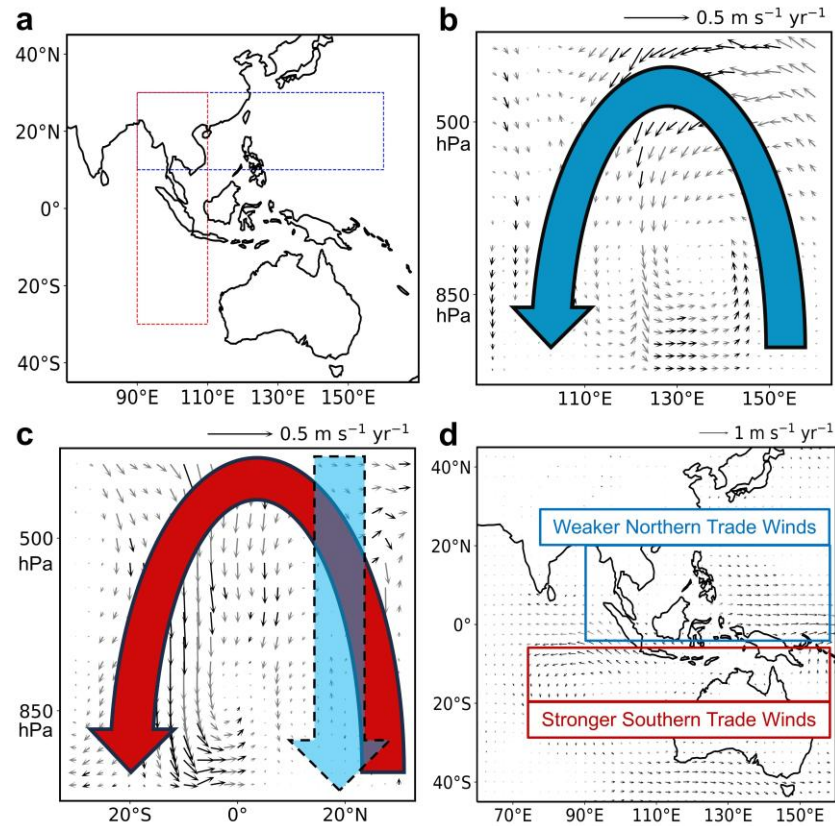240 similarities to the simulated results.

241

Figure R1. Linear trends in observed vertical circulations and 850 hPa wind fields in Asia-Pacific regions. Panel **b** and **c** shows pressure–longitude and latitude cross-section of linear trends in annual mean atmospheric circulations (unit: m s^{-1}, vectors) over areas marked with the blue and red box in panel **a** during 2010–2019 from ERA5. Panel **d** shows linear trends of wind fields (unit: m s^{-1}, vectors) at 850 hPa in Asia-Pacific regions. Trends of atmospheric circulations and winds which are statistically significant at the 90% confidence level are shown in black, while the insignificant ones are shown in grey.

249 My last comment regarding the figures is that the figure S15 should also be included in the main
250 text. It seems biased to try to find a link / attribution but only show the plots for China which the
251 authors have identified as the relevant one. Maybe a figure showing the annual precipitation trends
252 for CHN, OTH, NA+EU and then a seasonal plot for the CHN plots would be best?

As requested, we have moved the figure in the main text and showed the CHN, OTH, NA+EU (Figure 1 below) and then a seasonal plot for the CHN (Figure 2 below).
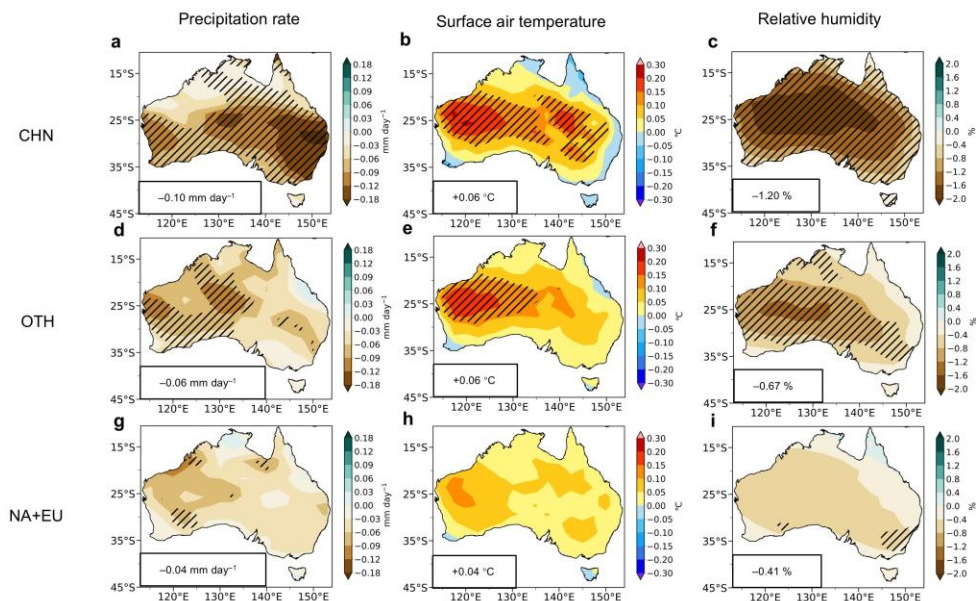

Figure 1. Simulated changes in precipitation rate, surface air temperature and relative humidity in Australia due to aerosol changes between 2013 and 2019. Spatial distributions of simulated differences in annual mean precipitation rate (Pr, **a**, **d,** and **g**, unit: mm day^{-1}), surface air temperature (TS, **b**, **e**, and **h**, unit: °C) and relative humidity (RH, **c**, **f**, and **i**, unit: %) in Australia between BASE and CHN (CHN minus BASE, **a–c**), between BASE and OTH (OTH minus BASE, **d–f**), and between BASE and NAEU (NAEU minus BASE, **g–i**). The shaded areas indicate results are statistically significant at the 90% confidence level. Regional averages over Australia are noted at the bottom-left corner of each panel.
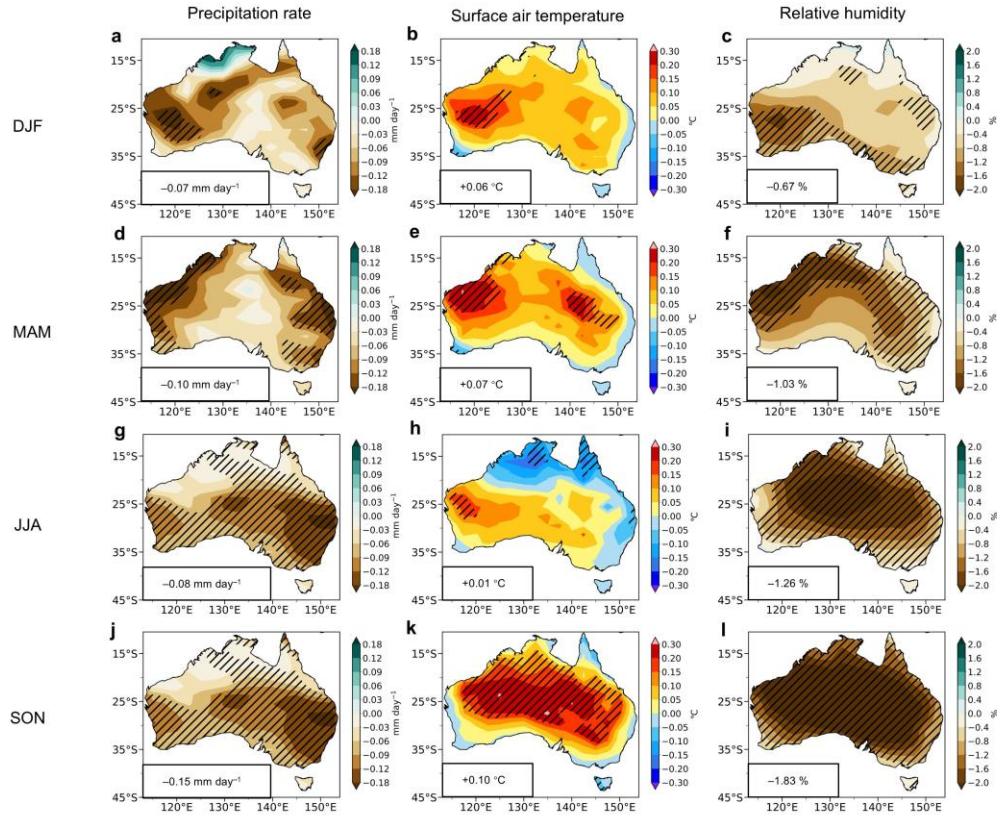
264

Figure 2. Simulated changes in precipitation rate, surface air temperature and relative humidity in Australia due to aerosol changes in China between 2013 and 2019. Spatial distributions of simulated differences in DJF (December, January and February, **a**–**c**), MAM (March, April and May, **d**–**f**), JJA (June, July and August, **g**–**i**) and SON (September, October and November, **j**–**l**) mean precipitation rate (Pr, **a**, **d**, **g**, and **j**, unit: mm day^{-1}), surface air temperature (TS, **b**, **e**, **h**, and **k**, unit: °C) and relative humidity (RH, **c**, **f**, **i**, and **l**, unit: %) in Australia between BASE and CHN (CHN minus BASE).The shaded areas indicate results are statistically significant at the 90% confidence level. Regional averages over Australia are noted at the bottom-left corner of each panel.

The authors discuss the influence of the (very strong) low bias in PM2.5 in CESM1 compared to the observations in L385-388, which is good and relevant. However, this should also be mentioned throughout the manuscript, for instance when the authors try to estimate very precise values for the influence of the Chinese aerosol reductions on precipitation and temperature (L270-271).

Thank you for your suggestion. We have made some corrections. While there is a low bias in PM$_{2.5}$ in CESM1 compared to observations, this is largely due to the model's inherently low background concentrations. Given that CESM1 has a relatively strong aerosol forcing due to strong aerosol-cloud interactions, the simulated climate effects may not have been significantly underestimated.

Minor comments

L29-31: The times mentioned in this sentence seem confusing since when first reading it seems

11

284 that a trend from 2013 is caused by something happening around the 2010s. Maybe using
285 "conditions since the 2010s" would help to settle this confusing sentence.

286 Revised.

287 L68-70: Please change "increasing GHGs" to increasing GHG emissions.

288 Changed.

289 L72-75: This sentence is very long and confusing, please split it up into two or shorten it

290 This sentence has been shortened as: "Atmospheric aerosols are the second-largest anthropogenic
291 climate forcer, exerting an overall cooling effect that partially masks the warming induced by
292 GHGs."

293 L73: "Earth's" instead of "earth's"

294 OK.

295 L104: "especially in northern Australia/especially in the North of Australia" instead of "especially
296 the northern Australia"

297 Revised.

298 L104: "affected by the Australian monsoon" instead of "affected by Australian monsoon"

299 Revised.

300 L153-159: Is there a reason for the choice of the GPM dataset rather than for instance GPCP data?

301 "GPM provides higher temporal and spatial resolution data compared to GPCP, making it more
302 suitable for studies focused on short-term precipitation variability and regional climate dynamics."
303 The statement has been added to the manuscript.

304 The GPCP data also exhibit a similar decreasing trend in precipitation over Australia, reinforcing
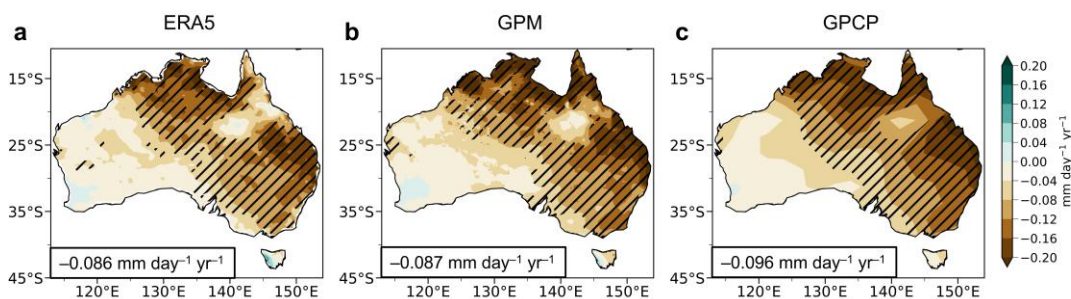305 the robustness of the observed trend (Figure S14).

306

307 **Figure S14. Linear trends of observed precipitation rate in Australia based on ERA5, GPM,**

308 **and GPCP.** Spatial distributions of linear trends annual mean precipitation rate (unit: mm day^{-1})
309 in Australia during 2010–2019 from ERA5 (a), GPM (b), and GPCP (c) datasets. The shaded areas
310 indicate trends are statistically significant at the 90% confidence level. Regional averages over
311 Australia are noted at the bottom-left corner of panels.

312 L224: "Earth's surface" instead of "earth's surface"

313 Revised.

314 L244: The setting of DF to 10 according to Sharples et al 2009 needs some more explanation. At
315 least one sentence why Sharples et al choose this value and why it is also applicable here.

316 Thank you for your suggestion. Sharples et al. (2009) mentioned that "Such a factor will have no
317 real bearing on the methods of comparison employed in the later sections of the paper and so for
318 convenience we assume that DF = 10 in what follows." We acknowledge that this assumption is
319 idealized. To address this, we have calculated gridded DFs (Figure S7 below) and found that the
320 DFs in Australia are close to 10, with spatial distributions being nearly homogeneous. Therefore,
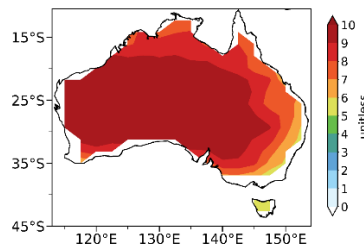321 setting DF = 10 for Australia is reasonable in this context.

322

323 **Figure S9. Spatial distributions of annual mean dry factor (unit: unitless) in Australia during**
324 **2010–2019.** The data is from fire danger indices historical data from the Copernicus Emergency
325 Management Service (CEMS, 2019; Vitolo et al., 2020).

326 Additionally, we compare FFDI with DF = 10 and FFDI with the gridded DF (Figure S8 below).
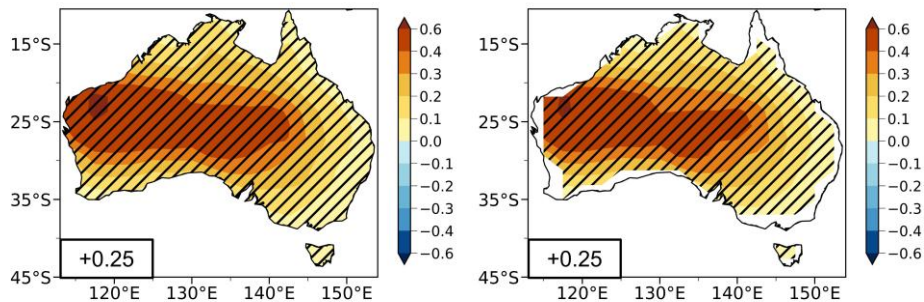327 The patterns and regional averages of both are similar.

328

329 **Figure S10. Spatial distribution of simulated changes in FFDI (unit: unitless) during fire**
330 **seasons in Australia between BASE and CHN (CHN minus BASE).** Shaded areas indicate
331 results that are statistically significant at the 90% confidence level. Regional averages for Australia

are noted at the bottom-left corner of each panel. The left panel shows FFDI (DF = 10), and the right panel shows FFDI (gridded DF).

L277: Please change "evidence" to "indication".

Changed.

L389: Please use "Earth System Model" or "fully-coupled climate model" instead of "aerosol-climate model" which would imply to me that this model is not fully coupled (which is the case according to the method section)

Thanks for your reminder. The term "aerosol-climate model" has been replaced with "fully-coupled climate model" throughout the manuscript, as suggested.

Figure S3: The colourbar of these two plots should be the same as the reader might be tricked into thinking that the magnitude changes between the observed and modelled data are similar.

Thank you for your suggestion. If we use the same color scale for both plots, the color range of the modeled results becomes overly uniform. However, we have now added a note in the figure caption to remind the reader that the magnitudes of the observed and modeled data are not directly comparable, and that the color scales represent different ranges.

References:

CSIRO and BOM: State of the Climate 2022, 2022

CEMS: Fire danger indices historical data from the Copernicus Emergency Management Service, https://doi.org/10.24381/cds.0e89c522, 2019.

Vitolo, C., Di Giuseppe, F., Barnard, C., Coughlan, R., San-Miguel-Ayanz, J., Libertá, G., and Krzeminski, B.: ERA5-based global meteorological wildfire danger maps, Sci. Data, 7, 216, https://doi.org/10.1038/s41597-020-0554-z, 2020.

Responses to Referee #2:

The manuscript investigates the role of the recent decline in East Asian anthropogenic aerosols in driving precipitation and temperature changes across Australia. The authors highlight the potential for aerosols to contribute to enhancing the fire risk via widespread drying and warming. The topic is timely and very important, as not many studies have examined the influence of recent changes in aerosols on recent climate variations. However, I find several major weaknesses in the study, including in the simulation design, that prevent the manuscript from being acceptable for ACPD. Unfortunately, I need to recommend a rejection. Happy though to reconsider the manuscript if reviewed accordingly.

Thank you for your feedback. We will carefully consider the points you raised regarding the simulation design and other aspects of the study. We value your insights and will make every effort to improve the quality of our work. We would be grateful for your reconsideration of the manuscript. Please see our point-by-point responses (in blue) to your comments below.

Major comments:

I believe there is a serious overinflation of the recent observed rainfall changes over Australia. Firstly, the authors use observations and plot linear trends from 2010, while model results are shown as 3-year differences from 2013. While the latter accounts for the decline in aerosols, observations show that the years 2010 and 2011 were anomalously wet over Australia, and just a couple of years before rainfall was much less (I have checked by plotting observations since 2000). This can also be inferred by examining Fig 2, where clearly the trend in panel d is affected by the two early years. By eye, using 3-year composites from 2013, the rainfall changes are very modest. Looking at more recent years, it turns out that 2019 was also anomalously dry, and more recent years (excluding those affected by COVID-related reduced emissions) show a recovery. Therefore the results based on observations, which ultimately is the motivation of the study, are strongly affected by the extremely short record and cannot be trusted.

Thank you for pointing out the strong variability in rainfall in Australia. We agree with reviewer that the observed trend of rainfall could be affected by the wet years in 2010/2011 and dry year in 2019, which could be induced by the interval variability (such as ENSO). However, we could not deny the decreasing precipitation during 2010–2019 and rule out the potential influence of changing aerosols on the rainfall variation. Additionally, we are trying to quantify the role of aerosol reduction in China in the Australian climate, rather than fully attribute to changing Australian climate to aerosols in China, considering that aerosol reductions in China are found to contribute to small part of the changing precipitation in Australia. The simulation results are still robust enough to support our conclusions because our model experiments are based on validated climate model, providing strong evidence that aerosol reductions in China have a significant impact on Australia's climate.

Additionally, to account for the potential influence of internal variability, particularly ENSO, which is a major driver of Australia's precipitation variability (Fig. S13), we have also adjusted the precipitation data by removing the influence of the Niño 3.4 index. The adjusted results exhibit a similar trend, confirming the robustness of the observed drying trend since the 2010s (Fig. S12)
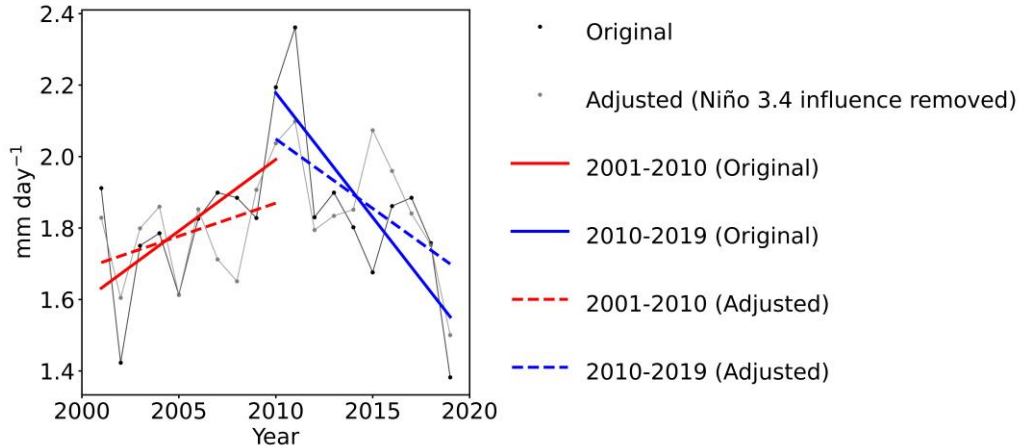
16

396

397
398
399
400

401

402
403
404

In fact, the emission reduction of aerosols and precursors in China starts in 2010 rather than 2013. We chose the year 2013 in simulation was because China implemented the "Air Pollution Prevention and Control Plan" in 2013 and established nationwide PM$_{2.5}$ observation sites in 2013. As the reviewer mentioned, Australia experienced a transient from dry years before 2010 to wet years in 2010/2011 and the rainfall recovery after 2020. It is also in accordance with the increasing aerosols in China before 2010 and the slowdown in aerosol reduction in recent years. But it still requires quantitative analysis.

405
406
407
408
409
410
411

Related to the point above, it is not surprising that observed circulation trends (e.g., Fig. S18) are extremely weak. Yet, this is the mechanism driving Australian rainfall changes, thus is central to

412
413

414 the proposed aerosol influence.

415 As mentioned earlier, given natural variability and the multiple factors influencing precipitation in
416 Australia, it is quite challenging to capture patterns in the observations that resemble the results of
417 the sensitivity experiment on China's aerosol reductions. We have redrawn the circulation figure
418 (Figure R1 below), displaying all circulations regardless of whether they pass the significance test.
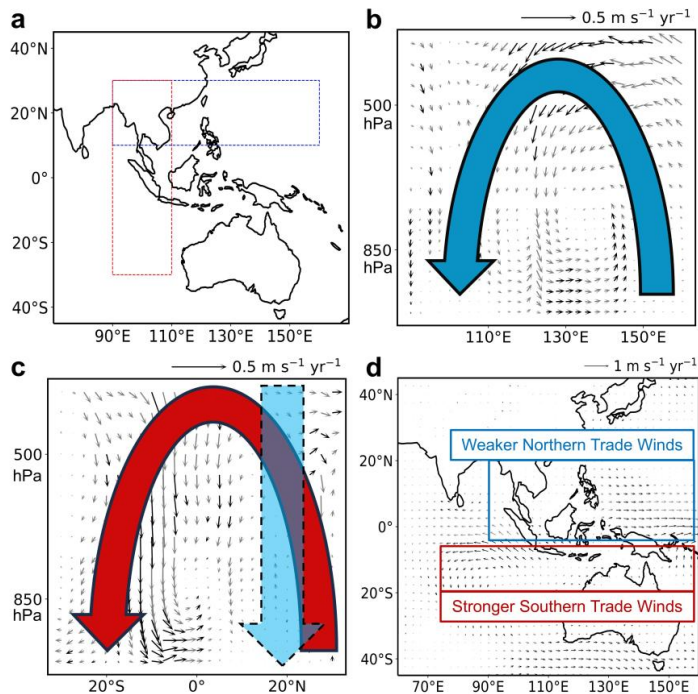419 Notably, we can observe clear similarities with the model results.

420

Figure R1. Linear trends in observed vertical circulations and 850 hPa wind fields in Asia-Pacific regions. Panel **b** and **c** shows pressure–longitude and latitude cross-section of linear trends in annual mean atmospheric circulations (unit: m s^{-1}, vectors) over areas marked with the blue and red box in panel **a** during 2010–2019 from ERA5. Panel **d** shows linear trends of wind fields (unit: m s^{-1}, vectors) at 850 hPa in Asia-Pacific regions. Trends of atmospheric circulations and winds which are statistically significant at the 90% confidence level are shown in black, while the insignificant ones are shown in grey.

428 The model analysis is also weak in the sense that 3-year composites are extremely short to identify
429 forced trends. In addition, observed trends should be first compared to those from a control
430 simulation and the contribution of aerosols should be related to the model world, not observations.

431 We believe there may be a misunderstanding regarding the 3-year composites mentioned by the
432 reviewer. In our study, we did not use 3-year composites for climate variables (only for PM$_{2.5}$ and
433 AOD in observations since they are more linear than climate variables). Our equilibrium
434 experiment designs have been described in the 2.2 Model Description and Experimental Design
435 section.

Regarding the model comparison, we would like to clarify that due to the nature of our equilibrium experiments, direct comparison with baseline control experiments is not feasible. Even in transient simulations, models may not be able to fully capture the short-term and complex observational signal, as observational data are influenced by numerous factors over short time periods. However, models can provide a qualitative evaluation of how specific factors, such as aerosols, might contribute to climate phenomenon. This approach has been commonly used in previous studies (Bollasina et al., 2011; Heede and Fedorov, 2021; Hwang et al., 2024; Vecchi et al., 2006; Wang et al., 2023; Yang et al., 2022) to isolate the impact of individual forcers.

While our simulations provide valuable insights into the physical mechanisms linking aerosol reductions to climate changes, we must admit that they cannot be intended for direct quantitative attribution of observed trends. **To clarify it, we have removed all statements that directly attribute the observed trend to the simulated aerosol response in a quantitative manner and now emphasize that the simulations serve as a tool for understanding the underlying processes rather than quantitatively estimating real-world aerosol-induced changes.** Moving forward, we recognize that transient simulations would be better suited for capturing short-term forced trends, and, we plan to incorporate them in future studies to further investigate the evolution of short-term responses and assess the potential contributions of other external forcings, such as greenhouse gases and internal variability.

Another major weakness is the experimental design. The authors examine long-term changes coming from equilibrium runs, which are far from representing the actual transient response over 10 years or so. This is likely far from being in equilibrium. I would have seen large-ensemble transient simulations with time-varying aerosols (2013-2024 for example) as more appropriate and suitable.

We appreciate the reviewer's concern regarding the use of equilibrium runs and the suggestion to use large-ensemble transient simulations. While transient simulations offer a more dynamic representation of temporal changes, the relatively short period from 2013 to the present may not provide enough time for the climate system to fully respond to aerosol changes. This is particularly true when considering the long timescales required for oceanic heat capacity to equilibrium. Furthermore, equilibrium simulations allow for a clearer isolation of the forced response to aerosol changes, minimizing the impact of short-term climate variability.

We do acknowledge, however, that transient simulations would offer a more accurate depiction of the time-varying effects of aerosol reductions, especially as aerosol reductions in China continue. As the climate system responds more robustly over time, transient simulations will likely become a more appropriate tool. Therefore, while equilibrium simulations are potentially more suitable for the present study, we plan to use transient simulations in future research.

We have also mentioned the limitation of not using transient simulations in the discussion section: "One limitation of this study is the use of equilibrium experiments. Although the equilibrium method is useful for isolating aerosol-induced climate responses, it does not fully capture the transient climatic evolution. Attributing observed climate changes directly to modeled aerosol-induced responses involves inherent uncertainties. Given the uncertainties, here we did not attempt to quantitatively attribute the observed climate change to aerosols in this study, but showed the mechanisms that how aerosol decline influence remote climate. Future work could also consider

478 transient simulations, which can better represent the role of aerosols in the climatic evolution of
479 the real world.".

480 Trends or changes should always be plotted with the related statistical significance, such as in Figs.
481 1 and 2.

482 Thank you for the suggestion. Now the indication of significance in all map figures has been
483 adjusted for improved clarity.

484 Fig 3: I think it would be more appropriate to display the divergent wind, rather than the total wind.

485 We chose to display the total wind in Figure 3 to highlight the strengthening of Southern Trade
486 Winds. For the divergent winds, we also displayed moisture divergence (Figure S18), which is
487 more directly related to the changes in precipitation patterns that we are investigating.

488

489 **References:**

490 Bollasina, M. A., Ming, Y., and Ramaswamy, V.: Anthropogenic Aerosols and the Weakening of
491 the South Asian Summer Monsoon, Science, 334, 502–505,
492 https://doi.org/10.1126/science.1204994, 2011.
493 Heede, U. K. and Fedorov, A. V.: Eastern equatorial Pacific warming delayed by aerosols and
494 thermostat response to CO_2 increase, Nat. Clim. Chang., 11, 696–703,
495 https://doi.org/10.1038/s41558-021-01101-x, 2021.
496 Hwang, Y.-T., Xie, S.-P., Chen, P.-J., Tseng, H.-Y., and Deser, C.: Contribution of anthropogenic
497 aerosols to persistent La Niña-like conditions in the early 21st century, Proc. Natl. Acad. Sci. U. S.
498 A., 121, e2315124121, https://doi.org/10.1073/pnas.2315124121, 2024.
499 Vecchi, G. A., Soden, B. J., Wittenberg, A. T., Held, I. M., Leetmaa, A., and Harrison, M. J.:
500 Weakening of tropical Pacific atmospheric circulation due to anthropogenic forcing, Nature, 441,
501 73–76, https://doi.org/10.1038/nature04744, 2006.
502 Wang, P., Yang, Y., Xue, D., Ren, L., Tang, J., Leung, L. R., and Liao, H.: Aerosols overtake
503 greenhouse gases causing a warmer climate and more weather extremes toward carbon neutrality,
504 Nat. Commun., 14, 7257, https://doi.org/10.1038/s41467-023-42891-2, 2023.
505 Yang, Y., Ren, L., Wu, M., Wang, H., Song, F., Leung, L. R., Hao, X., Li, J., Chen, L., Li, H., Zeng,
506 L., Zhou, Y., Wang, P., Liao, H., Wang, J., and Zhou, Z.-Q.: Abrupt emissions reductions during
507 COVID-19 contributed to record summer rainfall in China, Nat. Commun., 13, 959,
508 https://doi.org/10.1038/s41467-022-28537-9, 2022.

509

510

511
512

513 **Manuscript with tracked changes:**

514

515 **Dry and warm conditions in Australia exacerbated by aerosol reduction in China**

516

517

518

519

520 Jiyuan Gao[1], Yang Yang[1*], Hailong Wang[2], Pinya Wang[1], Hong Liao[1]

521

522

523

524

525

526

527

528 [1]Joint International Research Laboratory of Climate and Environment Change (ILCEC), Jiangsu

529 Key Laboratory of Atmospheric Environment Monitoring and Pollution Control, Jiangsu

530 Collaborative Innovation Center of Atmospheric Environment and Equipment Technology,

531 School of Environmental Science and Engineering, Nanjing University of Information Science

532 and Technology, Nanjing, Jiangsu, China

533 [2]Atmospheric, Climate, and Earth Sciences Division, Pacific Northwest National Laboratory,

534 Richland, Washington, USA

535

536

537

538

539

540 *Correspondence to yang.yang@nuist.edu.cn

541

Abstract

A substantial decline in anthropogenic aerosols in China has been observed since the initiation of clean air actions in 2013. Concurrently, Australia experienced anomalously dry and warm conditions ~~in~~since the 2010s. This study reveals a linkage between aerosol reductions in China and the drying and warming trends in Australia during 2013–2019 based on ~~aerosol~~ fully-coupled climate model simulations and multi-source observations. Aerosol decline in China triggered alterations in temperature and pressure gradients between the two hemispheres, leading to intensified outflow from Asia towards the South Indian Ocean, strengthening the Southern Indian Subtropical High and its related Southern Trade Winds. Consequently, this atmospheric pattern resulted in a moisture divergence over Australia. The reduction in surface moisture further resulted in more surface energy being converted into sensible heat instead of evaporating as latent heat, warming the near-surface air. Aerosol reductions in China are found to contribute to ~~19% of~~ the ~~observed~~ decreases in precipitation and relative humidity and ~~8% of~~ the increase in surface air temperature in Australia during 2013–2019. The intensified dry and warm climate conditions during 2013–2019 further ~~explain 12%–19% of~~caused the increase in wildfire risks during fire seasons in Australia. Our study illuminates the impact of distant aerosols on precipitation and temperature variations in Australia, offering valuable insights for drought and wildfire risk mitigation in Australia.

1 Introduction

Australia encompasses various climate zones, ranging from the tropical climate in the north to arid conditions in the interior and temperate climates in the south (Head et al., 2014). The continent is predominantly dry, receiving an average annual rainfall of less than 600 mm and less than 300 mm over half of the land. Evident long-term trends can be observed in Australia's historical rainfall records. These trends reveal a notable shift towards drier conditions across southern Australia (Dey et al., 2019a; Nicholls, 2006; Rauniyar and Power, 2020; Wasko et al., 2021), and an increase in rainfall before 2010 (Dey et al., 2019a, b; Evans et al., 2014; Nicholls, 2006; Rotstayn et al., 2007; Wasko et al., 2021) followed by a slight decreasing trend of rainfall after 2010 (CSIRO and BOM, 2022) in the northern Australia.

Precipitation in Australia is influenced by a variety of atmospheric circulation systems, including East Coast Lows (ECLs), the Australian-Indonesian Monsoon, tropical cyclones (TCs), fronts, and different modes of large-scale climate variabilities, such as the El Niño-Southern Oscillation (ENSO), Indian Ocean Dipole (IOD), Interdecadal Pacific Oscillation (IPO), Subtropical ridge (STR), Southern Annular Mode (SAM), and Madden Julian Oscillation (MJO) (Dey et al., 2019a; Risbey et al., 2009). The linkages between Australia's rainfall characteristics and these drivers could change in response to the internal natural variabilities and external anthropogenic forcings. Rauniyar and Power (2020) reported that the drier conditions across the southern Australia could be attributed to a combination of both decadal-scale natural variability and changes in large-scale atmospheric circulation patterns, which was linked to the escalating emissions of greenhouse gases (GHGs), while Rotstayn et al. (2007) found that the increased levels of rainfall in northern Australia before 2010 was linked to the increases in aerosols in Asia.

Human activities have led to a rise of global surface air temperature by approximately 1.29 °C (0.99 to 1.65 °C) from 1750 to 2019, mainly due to an enhanced greenhouse effect from increasing ~~GHGs~~GHG emissions (IPCC, 2021). In addition to GHGs, human activities also emit a variety of aerosols and their gaseous precursors into the atmosphere. Since industrialization, there has been a significant rise in the levels of aerosols and precursors (Hoesly et al., 2018). ~~These atmospheric~~Atmospheric aerosols ~~play a crucial role in changing the earth's radiation balance, both directly and indirectly, and are considered as~~are the second-largest anthropogenic climate

forcer ~~following GHGs~~, exerting an overall cooling effect that partially masks the warming induced by GHGs. (IPCC, 2013, 2021). However, as anthropogenic aerosols declined during the past decades in many countries of the world related to the clean air actions, the associated "unmask" effect is likely to exacerbate GHG-induced warming (Kloster et al., 2010). For example, in the 1980s, clean air actions were implemented in North America and Europe, leading to a decrease in the emissions of aerosols and their precursors (Hoesly et al., 2018). Reductions in aerosol emissions in the U.S. have led to changes in aerosol direct radiative forcing (DRF) by 0.8 W m^{-2} and indirect radiative forcing (IRF) by 1.0 W m^{-2} over the eastern U.S. during 1980–2010 (Leibensperger et al., 2012). Similarly, aerosol decreases over Europe between the 1980s and 1990s have caused a change in regional DRF by 1.26 W m^{-2} (Pozzoli et al., 2011). In China, the emissions of aerosols and their precursors have been reduced since 2013 due to the implementation of Air Pollution Prevention and Control Action Plan. Dang and Liao (2019) reported a 1.18 W m^{-2} change in DRF between 2012 and 2017 due to decreased aerosol levels over eastern China. Gao et al. (2022) estimated a warming of 0.20 °C in China, 0.15 °C in North America, and 0.14 °C in Europe, attributed to the decreases in aerosols during 2013–2019.

Monsoonal rainfall serves as a vital resource for agriculture, industry, and ecosystems across the monsoon-affected regions, affecting approximately two-thirds of the world's population (B. Wang et al., 2021). Apart from GHGs-induced warming (Cook and Seager, 2013) and nature variabilities (e.g., ENSO) (Oh and Ha, 2015), aerosol also modulates monsoon system mainly through changing land-sea temperature and pressure gradient. The impact of aerosols on Asian monsoon has been widely investigated. Based on climate model simulations, Liu et al. (2023) found that aerosol reductions in East Asia during 2013–2017 resulted in an approximately 5% increase in the strength of the East Asian summer monsoon (EASM). The EASM is also reported to enhance due to future aerosol reductions from 2000 to 2100 (Wang et al., 2016). Dong et al. (2019) explored the effects of increased aerosol in Asia from 1970s to 2000s on atmospheric circulation and rainfall patterns and found anomalous moisture convergence and increased precipitation over the Maritime continent. Non-Asian aerosols also have an effect on South Asian monsoon rainfall through changes in the interhemispheric temperature gradient and meridional shifts of the Intertropical Convergence Zone (Bollasina et al., 2011, 2014; Cowan and Cai, 2011; Undorf et al., 2018). Australia, especially ~~the~~in northern Australia, is largely affected by the Australian monsoon, which is characterized by winds that blow from the southeast during cold

621 season and from the northwest during the warm season (Gallego et al., 2017; Heidemann et al.,
622 2023). Australia has a relatively low level of anthropogenic aerosols, which suggests that the
623 impact of domestic anthropogenic aerosols on Australian monsoon should not be significant.
624 However, the impact of remote aerosols on Australian monsoon have been investigated in previous
625 studies, and they reported that the increases in Asian aerosols could enhance rainfall in Australia
626 through increasing monsoonal winds towards Australia (Rotstayn et al., 2007; Fahrenbach et al.,
627 2023).

628 Wildfires, which are uncontrolled fires spreading rapidly across natural landscapes, are
629 significantly influenced by meteorological conditions (He et al., 2019; Jones et al., 2022). In
630 Australia, these fires, also known as bushfires, present a major environmental and social threat
631 (Johnston et al., 2021; Ward et al., 2020). According to Dowdy (2020), the most favorable seasons
632 for wildfires in most regions of Australia are austral spring and summer. Key meteorological
633 factors such as extended periods of drought, elevated temperatures, low humidity, and strong winds
634 are crucial in determining the occurrence and intensity of wildfires (Zacharakis and Tsihrintzis,
635 2023). Under the recent historical climate change, Australia has witnessed a rise in extreme fire
636 weather conditions and an extended fire season (CSIRO and BOM, 2022).

637 Since the implementation of clean air policies in 2013, there has been a noticeable decrease
638 in aerosol levels in China (Zhang et al., 2019; Zheng et al., 2018). Numerous studies have shown
639 the local and global climate effects of the aerosol reductions in China (Dang and Liao, 2019; Gao
640 et al., 2022, 2023; Liu et al., 2023; Zheng et al., 2020). The Australian monsoonal wind patterns,
641 reported to be influenced by Asian aerosol emissions in the past decades (Rotstayn et al., 2007;
642 Fahrenbach et al., 2023), may have also influenced by the radiative effects due to the aerosol
643 decline in China. The objective of this study is to assess the worsened dry and warm conditions
644 and associated wildfire risk in Australia during 2013–2019 and investigate the possible linkage
645 between the changes in climate conditions in Australia and anthropogenic aerosols.

646 **2 Methods**

647 **2.1 Observational and Reanalysis Data**

648 Ground-based observational data of near-surface $PM_{2.5}$ concentrations in China 2013–2019

are acquired from the China National Environmental Monitoring Centre (CNEMC), which offers daily records of near-surface air pollutant concentrations for nearly 1800 sites. Aerosol Optical Depth (AOD) data are obtained from the Moderate Resolution Imaging Spectroradiometer (MODIS) Deep Blue retrieval (Hsu et al., 2013). These observational data are used for evaluating the performance of model simulated aerosols.

ERA5, the fifth generation of the European Centre for Medium-range Weather Forecasts (ECMWF) atmospheric reanalysis, is a comprehensive dataset that provides a detailed and globally consistent view of the earth's atmospheric conditions over the past several decades (Hersbach et al., 2020). In this study, ERA5 data are employed to evaluate the climate condition in Australia and analyze its linkage with aerosol reductions in China during the 2013–2019 by using the 2-meter temperature, total precipitation, relative humidity, cloud cover, wind fields, vertical velocity, surface latent and sensible heat flux, and surface and top of the atmosphere (TOA) solar and longwave radiative flux under both clear and all sky conditions.

Clouds and the Earth's Radiant Energy System-Energy Balanced and Filled (CERES-EBAF) is a dataset that provides information on the earth's radiation budget, including surface and TOA energy fluxes (Loeb et al., 2018). It combines data from satellite instruments to estimate how much energy the earth receives from the sun and how much is reflected back to space, helping to understand climate change and energy balance processes. The variables used in the study include cloud cover and surface and TOA solar and longwave radiative fluxes under both clear and all sky conditions.

The Global Precipitation Measurement (GPM) mission is a joint initiative by National Aeronautics and Space Administration (NASA) and the Japan Aerospace Exploration Agency (JAXA) aimed at providing accurate and frequent measurements of global precipitation (Skofronick-Jackson et al., 2017). GPM includes a core satellite equipped with advanced radar and microwave sensors, enabling the observation of rain and snowfall in real-time. The data are crucial for understanding weather patterns, climate dynamics, and hydrological processes. The Global Precipitation Climatology Project (GPCP) is an international initiative under the World Climate Research Programme (WCRP) that integrates satellite and gauge-based observations to provide long-term, global precipitation estimates (Adler et al., 2018). Precipitation rate data from GPM are

678 ~~also used in the study~~GPCP offers monthly and daily precipitation datasets with global coverage,
679 combining data from rain gauges, satellite infrared (IR), and microwave sensors to enhance
680 accuracy. Precipitation rate data from GPM and GPCP are also used in the study. GPM provides
681 higher temporal and spatial resolution data compared to Global Precipitation Climatology Project
682 (GPCP), making it more suitable for studies focused on short-term precipitation variability and
683 regional climate dynamics.

684 **2.2 Model Description and Experimental Design**

685   In this research, we conduct simulations to explore the impact of aerosols on climate using
686 the Community Earth System Model version 1 (CESM1). CESM1 simulates the major aerosols
687 including sulfate, black carbon (BC), primary organic matter (POM), secondary organic aerosol
688 (SOA), dust and sea salt in a four-mode Modal Aerosol Module (MAM4), as described in Liu et
689 al. (2016). CESM1 simulations are carried out with 30 vertical layers and a horizontal resolution
690 of 2.5° longitude by 1.9° latitude. In addition to the default model physics, several supplementary
691 features are incorporated into the model in this study to improve the model's performance in
692 simulating aerosol wet scavenging and convective transport (Wang et al., 2013).

693   The global anthropogenic emissions of aerosols and their precursors are obtained from the
694 Community Emissions Data System (CEDS) v_2021_04_21. In contrast to the prior CEDS
695 v_2016_07_26, which exhibits significant regional emission biases (Z. Wang et al., 2021), the
696 newer CEDS version of anthropogenic emissions of aerosols and precursors considers the
697 substantial reductions in emissions in China, related to the recent clean air actions since 2013 (Fig.
698 S1). Specifically, anthropogenic sulfur dioxide (SO_2), BC, and organic carbon (OC) emissions
699 decreased by −12.48, −0.30, and −0.21 Tg yr^{-1}, respectively, over China between 2013 and 2019.
700 Biogenic emissions are from the Model of Emissions of Gases and Aerosols from Nature version
701 2.1 (MEGAN v2.1) (Guenther et al., 2012), while the emissions from open biomass burning are
702 derived from the CMIP6 (Coupled Model Intercomparison Project Phase 6) (Van Marle et al.,
703 2017).

704   A series of model experiments are conducted using CESM1 with a fully-coupled model
705 configuration, as detailed in Table S1. In the baseline scenario (referred to as BASE),
706 anthropogenic emissions of aerosols and precursors are fixed at year 2013 worldwide. In CHN,

707   anthropogenic emissions of aerosols and precursors over China are fixed at year 2019, while

708   emissions in all other regions are remained at year 2013. In NAEU, the simulation is performed

709   with anthropogenic emissions of aerosols and precursors over North America and Europe set at

710   year 2019, while emissions in other regions remained at year 2013. In OTH, anthropogenic

711   emissions of aerosols and precursors in other regions except for China are set at year 2019, while

712   emissions in China are kept at year 2013. Biogenic and biomass burning emissions worldwide in

713   all experiments are fixed at year 2013. To reduce model biases related to internal variability, three

714   ensemble members are conducted by perturbing the initial atmospheric temperature conditions.

715   All simulations are run for 150 years, with the last 100 years for detailed analysis.

716   **2.3 Model Evaluation**

717   To validate whether CESM1 can reproduce the aerosol reductions in China during the 2010s,

718   changes in simulated near-surface $PM_{2.5}$ concentrations (sum of sulfate, BC, POM, SOA, dust×0.1,

719   and sea-salt×0.25 following Turnock et al. (2020)) in China during 2013–2019 are compared with

720   the observations. Figure S2 shows spatial distributions of observed and modeled annual mean near-

721   surface $PM_{2.5}$ concentration changes over China (2017–2019 minus 2013–2015), which exhibited

722   a statistically significant correlation coefficient of 0.52 between simulations and observations.

723   However, the model underestimates the $PM_{2.5}$ concentration changes by 76% in China. The

724   considerable underestimation has been reported in many previous studies, resulting from coarse

725   model resolution, uncertainties in emissions of aerosols and precursor gases, strong aerosol wet

726   removal, and the model's deficiency in simulating nitrate and ammonium aerosols (Fan et al., 2018,

727   2022; Gao et al., 2022, 2023; Zeng et al., 2021). The model has a good capability in replicating

728   the spatial distribution of AOD changes in China during 2013–2019 (Fig. S3), as evidenced by a

729   high correlation coefficient of 0.83, but the model also exhibits an underestimation in the AOD

730   reductions by 69%. However, the apparent underestimation of absolute changes may largely stem

731   from the inherently low background aerosol concentrations in CESM1. When considering the

732   relative changes rather than absolute values, the bias appears much less pronounced (Fig. S4 and

733   Fig. S5).

734   Climate variables, including precipitation rate, surface air temperature, relative humidity,

735   total cloud cover, surface solar radiation, 10m wind speed, and surface and TOA net total radiative

28

736 fluxes under both clear and all sky conditions over Australia simulated by CESM1 model are also

737 compared with those from ERA5 reanalysis (Fig. ~~S4~~ S6 S8). The model demonstrates a good

738 performance in simulating Australian climate, with normalized mean bias (NMB) values

739 consistently below or near 40% for surface air temperature, relative humidity, total cloud cover,

740 surface downward solar radiation, and 10m wind speed, and surface and TOA net total radiative

741 fluxes, but it tends to overestimate annual precipitation by about 90%, especially over coastal

742 regions likely related to the coarse model resolution. The model accurately reproduces spatial

743 patterns of all climate variables, closely aligning with observations, as indicated by correlation

744 coefficients ranging from 0.7 to 1.0.

745 **2.4 Wildfire Risk Indices**

746 In this study, several climatological indices are used to indicate wildfire risk during fire

747 seasons (austral spring and summer, from September to February of the next year) in Australia

748 (Ren et al., 2022; Irmak et al., 2003; Seager et al., 2015; Sharples et al., 2009).

749 (i) Reference Potential Evapotranspiration (ET_0):

750 ET_0 is a climatological index used to estimate the amount of water that could potentially

751 evaporate and be transpired from the ~~earth's~~ Earth's surface under specific meteorological

752 conditions. The calculation of ET_0 takes into account factors such as temperature (T, unit: °C), and

753 surface downward solar radiation (R_s, unit: W m^{-2}) to estimate the maximum amount of water loss

754 due to evaporation and transpiration. ET_0 is important in wildfire studies because it helps to gauge

755 the environmental moisture conditions and the potential for drought, which can be a significant

756 factor in wildfire risks assessment. ET_0 is given by the following expression (Irmak et al., 2003):

$$ET_0 = -0.611 + 0.149R_s + 0.079\text{T}$$

758 (ii) Vapor Pressure Deficit (VPD):

759 Vapor Pressure Deficit (VPD) is a meteorological parameter that measures the difference

760 between the amount of moisture in the air and the maximum amount of moisture the air can hold

761 at a given temperature (T, unit: °C) and moisture (relative humidity, RH, unit: %). High VPD

762 values indicate that the air is dry. VPD is important in the context of wildfires because it reflects

the drying potential of the atmosphere. When VPD is high, it can lead to rapid moisture loss from vegetation, making it more susceptible to ignition and increasing the risk of wildfires. VPD is given by (Seager et al., 2015):

$$VPD = \frac{100 - RH}{100} \times 610.7 \times 10^{\frac{7.5T}{237.3+T}}$$

(iii) McArthur Forest Fire Danger Index (FFDI):

The McArthur Forest Fire Danger Index (FFDI) is a widely used index in Australia to assess the potential for bushfires and forest fires. It takes into account various meteorological factors, including T (unit: °C), RH (unit: %), wind speed (U, unit: m s^{-1}), and drought factor (DF, unitless). We set DF as 10 here following Sharples et al. (2009).(2009), as it would not significantly affect the methods of comparison used later in their study. While we acknowledge that this assumption is idealized, we find it applicable in our case. To verify this, we calculated gridded DFs for Australia (Figure S9), which show that the DFs are close to 10 and exhibit nearly homogeneous spatial distributions. As such, setting DF = 10 for Australia is reasonable for our analysis. In addition, FFDI calculated using DF = 10 and FFDI using gridded DFs are compared (Figure S10). The patterns and regional averages of both datasets are very similar, further supporting the use of DF = 10 in our study. The FFDI provides a numerical rating that indicates the level of fire danger, with higher values corresponding to greater fire risks. This index is particularly valuable for assessing the immediate risk of wildfires and is commonly used in fire management and prediction. FFDI is defined as (Sharples et al., 2009):

$$FFDI = 2e^{-0.45+0.987lnDF+0.0338T-0.0345RH+0.0234U}$$

3 Results

3.1 Intensified Dry and Warm Conditions in Australia by aerosol changes

Figure 1 shows simulated responses in annual and seasonal precipitation rate, surface air temperature and relative humidity in Australia to changes in anthropogenic emissions of aerosols and precursors in China. In response to aerosol reductions in China, Australia experiences significant decreases in precipitation and relative humidity, while the temperature has an increase

789 from 2013 to 2019. On regional average, annual precipitation, surface air temperature and relative

790 humidity change by –0.10 mm day^{-1}, 0.06 °C, and –1.20%, respectively, in Australia caused by

791 the aerosol reduction in China during this time period, contributing to the dry and warm climate in

792 Australia. Notably, Northern Australia experiences the most significant reduction in convective

793 precipitation, whereas Southern Australia has the greatest decline in large-scale precipitation

794 related to the aerosol reduction in China, as simulated by the CESM1 model (Fig. ~~S7~~S11). The

795 direction of seasonal responses in precipitation rate, surface air temperature and relative humidity

796 are the same as the annual averages, with the largest changes occurring in austral spring (Fig. ~~1~~2).

797   The intensified dry and warm conditions in Australia can also be seen in the observations,

798 as indicated by ERA5 reanalysis data (Fig. ~~2).~~3). Since 2010, precipitation and relative humidity

799 have significantly decreased in Australia, especially in Northern and Eastern Australia, at a rate of

800 0.086 mm day^{-1} yr^{-1} and 1.07% yr^{-1}, respectively, while surface air temperature has increased at a

801 rate of 0.17 °C yr^{-1}. ~~The decrease in precipitation in Australia is also reflected in the GPM data~~

802 ~~(Fig. S8). It translates into the changes in precipitation, temperature and relative humidity by 0.52~~

803 ~~mm day^{-1}, 1.0 °C and 6.4% in Australia during 2013–2019 in observations if the trends are~~

804 ~~assumed to be linear. This suggests that aerosol reductions in China can explain 19% of the~~

805 ~~decreases in precipitation and relative humidity and 8% of the increase in surface air temperature~~

806 ~~in Australia during 2013–2019, worsening the dry and warm climate conditions in Australia (Fig.~~

807 ~~S9).~~In addition, Time series of precipitation have also been extended to cover 2001–2019, clearly

808 showing an increasing precipitation trend during 2001–2010, followed by a decreasing trend

809 during 2010–2019 (Fig. S12). It is in accordance with the increasing aerosols in China before 2010

810 and aerosol reduction in recent years. To account for the potential influence of internal variability,

811 particularly ENSO, which is a major driver of Australia's precipitation variability (Fig. S13), the

812 time series are also given after removing the influence of Niño 3.4 index. The adjusted results

813 exhibit a similar transition, confirming the robustness of the observed drying trend since the 2010s

814 (Fig. S12). The GPM and GPCP data also exhibit a similar decreasing trend in precipitation over

815 Australia (Fig. S14). The reduction in anthropogenic SO$_2$ emissions in China shows strong

816 correlations with the decrease in precipitation and the increase in temperature in Australia during

817 2010–2019 (Fig. ~~S10~~S15). However, when extending the time frame to the period before emissions

818 reductions in China (1940–2019), the increase in temperature becomes less pronounced, with a

819 slight rise in precipitation and relative humidity, likely attributed to greenhouse gas warming,

which can serve as ~~evidence~~indication that the decrease in precipitation and increase in temperature in Australia from 2010 to 2019 are not primarily caused by GHGs (~~Figure S11~~Fig. S16). The rainfall decrease is consistent with changes in clouds. Spatial distributions of simulated changes in vertically-integrated cloud cover ~~and the linear trends in observations are shown in Fig. S12–S14. In both observation and model simulation, the results consistently indicate~~are shown in Figure S17, indicating a reduction in clouds of all levels, including high, mid-level, and low clouds. In addition, the spatial distributions of these changes closely resemble the patterns of responses in precipitation and relative humidity.

Aerosol emissions have changed across the world rather than in China alone during 2013–2019, such as those in Australia, North America and Europe, which affect climate in both local and remote regions. ~~Figures S15a and S15b~~Figure 1 also shows changes in ~~precipitation and surface temperature~~climate variables in Australia due to changes in other regions except China. The aerosol changes in other regions except China yield a decrease in precipitation by 0.06 mm day^{-1} ~~and~~, an increase in temperature by 0.06 °C~~, which are similar to those caused~~ and a decrease in relative humidity by ~~the aerosol changes in China (Fig. 1).~~0.67%. In particular, North America and Europe emission changes ~~largely~~, to some extent, contribute to the responses in precipitation (–0.04 mm day^{-1} ~~) and~~), temperature (0.04 °C) and relative humidity (–0.41%) attributed to other regions (except China), although the responses are mostly insignificant (~~Figs. 15c and 15d~~Fig. 1).

3.2 Mechanisms of Dry and Warm conditions in Australia Amplified by Aerosol Reductions in China

The rising levels of Asian aerosols could influence the meridional temperature and pressure gradients across the Indian Ocean and therefore affect monsoonal winds and rainfall in Australia since the middle of the 20th century, as reported in several previous studies (Fahrenbach et al., 2023; Rotstayn et al., 2007). Since 2013, aerosol levels in China have substantially decreased due to clean air actions initiated by the Chinese government (Zhang et al., 2019). At the same time, precipitation in Australia exhibited a declining trend, which could be partly attributed to the decrease in China's anthropogenic aerosol forcing as quantified through CESM1 simulations.

Asian monsoon region is closely connected with the meridional Hadley circulation and zonal Walker circulation through monsoon outflow to the South India ocean subtropical high (SISH) and

849 North Pacific subtropical high (NPSH) (Beck et al., 2018). Figure ~~S16~~4a illustrates the

850 climatological mean wind fields at 850 hPa, indicating the persistent existence of SISH in the

851 Indian Ocean and NPSH in the North Pacific. With reductions in aerosols in China, the sea surface

852 temperature (SST) increases in the North Pacific but decreases in the Indian Ocean (Fig. ~~S17~~4b),

853 which is concurrent with the northward shift of the Intertropical Convergence Zone (ITCZ) (Basha

854 et al., 2015). Over Asia, this migration of ITCZ is accompanied by the northward movement of

855 the upper-tropospheric subtropical zonal westerly jet (Chiang et al., 2015; Schiemann et al., 2009),

856 which moves to the north of the Tibetan Plateau. It then enhances the circulation pattern of the

857 Tibetan high, redirects the outflow from the Asian monsoon to the southern Indian Ocean

858 subtropical high (Fig. ~~3e~~5c), strengthens the SISH, and leads to the enhancement of the Southern

859 Trade Winds (Fig. ~~3d~~5d). On the other hand, the increase in SST in the North Pacific induces

860 ascending motion around the 130°–150°E and the subsequent descending motion around the 90°–

861 110°E (Fig. ~~3b~~5b), with anomalous westerly winds near the surface, leading to a weakening of

862 NPSH along with a decrease in the Northern Trade Winds (Fig. ~~3d~~5d). Note that, the descending

863 motion partly compensates the ascending motion related to the meridional circulation between

864 10°–30°N (Fig. ~~3c). Similar changes of vertical and horizontal circulations are also shown in the~~

865 ~~real world in the 2010s (Fig.~~ 5c). The mechanism of China's aerosol reductions on the large-scale

866 3D circulation in the Asia-Pacific region is shown in Figure 6.~~S18).~~ The enhancement of the

867 Southern Trade Winds further causes moisture advection away from Australia, accompanied by

868 moisture divergence in Australia, especially over the northern Australia (Fig. S18).~~S19). Moisture~~

869 ~~divergence is also evident in the observations for some northern regions of Australia (Fig. S20).~~

870 This moisture divergence in Australia then intensifies the dryness in Australia ~~both in CESM1~~

871 ~~simulations~~ (Fig. 1~~) and ERA5 reanalysis (Fig. 2~~).

872   Figures ~~S21~~7 illustrate the changes in relevant radiative fluxes in Australia resulting from

873 aerosol changes in China. Under the clear sky condition, both surface and top of the atmosphere

874 (TOA) radiative flux decrease (Fig. ~~S21e~~7c&d). It is due to increased sea salt and dust aerosols

875 (Fig. ~~S22b~~S19b–d) due to the stronger Southern Trade Winds (Figs. ~~S22a~~S19a and ~~3d~~5d) and dryer

876 conditions (Fig. ~~1a&e~~1). The decrease in cloud cover (Fig. ~~S12~~S17) leads to an overall increase in

877 both surface and TOA radiative flux (Fig. ~~S21e~~7e&f). The overall changes in radiative fluxes are

878 offset by these two factors (Fig. ~~S21a~~7a&b) and insufficient to explain the significant increase in

879   surface air temperature in Australia (Fig. ~~1b). Similar signals are also evident in the observational~~
880   ~~data represented by ERA5 and CERES-EBAF (Figs. S23 and S24~~1).

881   Decreases in precipitation lead to a decrease in surface specific humidity (Fig. ~~S25a~~S20a),
882   which declines more than that at 850 hPa (Fig. ~~S25b~~S20b). This results in excess energy being
883   converted into sensible heat rather than latent heat through evaporation (Chiang et al., 2018;
884   Fischer et al., 2007; Seneviratne et al., 2006; Su et al., 2014), which is indicated by a decrease in
885   surface upward latent heat flux and an increase in surface upward sensible heat flux in Australia
886   due to aerosol changes in China in Figure ~~S26~~8. The increased surface upward sensible heat flux
887   heats the near-surface air and contributes to the warm conditions in Australia. ~~The signals of~~
888   ~~specific humidity and surface sensible/latent heat flux from ERA5 are consistent with the~~
889   ~~simulated results. (Figs. S27 and S28).~~

890   **3.3 Increases in Wildfire Risk in Australia**

891   Wildfires represent a biosphere-atmosphere phenomenon, arising from the intricate interplay
892   of weather, climate, fuels, and human activities (Moritz et al., 2014). Notably, wildfires are ranked
893   among the most significant natural disasters in Australia, causing extensive damage (Shi et al.,
894   2021). Collins et al. (2022) reported that warmer and drier conditions increased the potential for
895   large and severe wildfire in Australia. Given that changes in aerosols in China have led to a warmer
896   and drier climate condition in Australia in recent years, the change in this climate state could also
897   impact on the occurrence of wildfires. Three wildfire risk indices (ET_0, VPD, and FFDI) are
898   selected to assess the risks of wildfires occurrence. Detailed information about the three wildfire
899   risk indices can be found in the Methods section.

900   All three indices exhibit increases (+0.37 mm mon^{-1} for ET_0, +0.56 hPa for VPD, and +0.25
901   for FFDI) during fire seasons (September to February) in Australia due to changes in aerosols in
902   China during 2013–2019 (Fig. ~~4~~9), although they do not show the same spatial distribution
903   possibly due to different considerations regarding climate variables in the indices. ~~The results~~
904   ~~analyzed from observational data also exhibit increasing trends at a rate of 0.32 mm mon^{-1} yr^{-1} for~~
905   ~~ET_0, 0.59 hPa yr^{-1} for VPD, and 0.34 yr^{-1} for FFDI during this time period (Fig. S29). It further~~
906   ~~indicates that the decline in anthropogenic aerosols in China can explain 12%–19% of the increase~~

in wildfire risks during the fire season in Australia between 2013 and 2019 through inducing dry and warm wildfire weather conditions (Fig. S9).

4 Conclusions and Discussions

This study reveals a plausible connection between the substantial aerosol reduction in China and drying and warming trends in Australia that happened during the 2010s. Aerosol reductions in China induce changes in temperature and pressure gradients, which lead to an increased outflow from Asia towards the South Indian Ocean, strengthening the SISH and the associated Southern Trade Winds. Consequently, this atmospheric pattern results in moisture divergence over Australia, causing a decrease in humidity and precipitation. The reduction in surface moisture leads to more surface energy being converted into sensible heat, rather than evaporating as latent heat, thereby heating the near-surface air. This perspective sheds light on the influence of distant aerosols on climate in Australia.

The CESM1 simulations depict warmer and drier conditions in Australia related to China's aerosol reductions than otherwise, a pattern also evident in observations represented by ERA5. However, it is important to note that China's aerosol reductions only contribute to a portion of the observed warm and dry conditions in Australia. According to the CESM1 simulations, aerosol changes in China account for 19% of the observed decrease in relative humidity and precipitation and 8% of the increase in temperature in Australia throughout the year, and 12% 19% of the increase in wildfire risks during the fire season in Australia during 2013 2019. Nonetheless, air quality and human health improvements owing to aerosol reductions cannot be ignored (Giani et al., 2020; Zheng et al., 2017). In addition, the drying and warming trends in Australia attributed to aerosol reductions should be considered resulting from the rise in long-lived GHGs, while the aerosol reductions unmask the effect rooted in the GHGs (Wang et al., 2023). In addition, other factors such as internal climate variability (Heidemann et al., 2023) appear to have contributed more to the changes in Australia's climate conditions.

Rotstayn et al. (2007) and Fahrenbach et al. (2023) investigated the impact of increasing anthropogenic aerosols over Asia during the late 20th century and early 21st century and indicated that enhanced aerosol emissions strengthened the meridional temperature and pressure gradients, intensifying the monsoonal circulation and leading to increased precipitation over Australia. In

35

contrast, our study focuses on the recent reductions in anthropogenic aerosols in China since 2013, showing that the aerosol reductions reversed circulation changes induced by the previous aerosol increases and contributed to drying rather than increased rainfall over Australia. Our study also explores the subsequent impact of aerosol reductions in China on Australian temperature. We find that reduced moisture availability over Australia led to a shift in surface energy partitioning, with more energy being converted into sensible heat rather than latent heat, resulting in near-surface warming. In summary, while previous studies have demonstrated the role of increasing Asian aerosols in enhancing Australia's precipitation, our work complements these findings by showing that decreasing aerosols, particularly from China, can drive the opposite effect, contributing to both drying and warming conditions in Australia.

One limitation of this study is the use of equilibrium experiments. Although the equilibrium method is useful for isolating aerosol-induced climate responses, it does not fully capture the transient climatic evolution. Attributing observed climate changes directly to modeled aerosol-induced responses involves inherent uncertainties. Given the uncertainties, here we did not attempt to quantitatively attribute the observed climate change to aerosols in this study, but showed the mechanisms that how aerosol decline influence remote climate. Future work could also consider transient simulations, which can better represent the role of aerosols in the climatic evolution of the real world.

There are some other potential ~~limitations and~~ uncertainties in this study. Firstly, the low bias in simulated aerosol concentrations in CESM1 ~~could potentially lead to an underestimation of the climate responses in Australia, and the extent to which the low bias~~ and CESM1's larger sensitivity to aerosol forcing could ~~influence the results remains unknown.~~ introduce some uncertainties. Secondly, our findings are derived from simulations conducted with a single ~~aerosol~~ fully-coupled climate model, and it is vital for future research to employ multi-model ensemble simulations to reduce the possibility of model-dependent specific results. While the CMIP6 and PDRMIP (Precipitation Driver Response Model Intercomparison Project) can assist in minimizing such model dependencies, they also present certain drawbacks. Anthropogenic emissions input in CMIP6 inadequately accounts for aerosol reductions resulting from clean air actions in China since 2013 (Z. Wang et al., 2021). Additionally, CMIP6 considers aerosol changes globally, making it challenging to isolate effects specifically induced by changes in aerosols in China. The

experimental design of PDRMIP, which scales the concentrations of sulfate and BC in Asia to ten times of their present-day levels, is generally idealistic and may not accurately and proportionally represent aerosol changes observed in the real world. ~~Until now, few studies have explored the link between the recent reduction in China's aerosols and the changing climate conditions in Australia. Although Fahrenbach et al. (2023) investigated the connection between increased precipitation in Australia and elevated aerosol levels in Asia since the last century, they focused on the decadal time scale with historical increasing aerosols in Asia.~~ Finally, in addition to aerosols, GHGs and nature variabilities also contribute to regional and global climate change. The extent to which GHGs and nature variabilities could contribute to weather condition and climate changes in Australia remains unknown, which warrants further investigation.

Nonetheless, our study examined the role of China's aerosol reductions in Australia's recent drying and warming trends. Substantial emission reductions will continue in China following the carbon neutral pathway (Yang et al., 2023), while future changes in emissions in South Asia remain uncertain (Samset et al., 2019). Apart from natural climate variabilities that affect the Australian monsoon, further investigation of changes in monsoon precipitation in Australia should also consider the effects of remote aerosol changes simultaneously, which is crucial to effective drought and wildfire management and mitigation in Australia.

Acknowledgments

Data and Code Availability

Ground-based observed $PM_{2.5}$ concentrations from CNEMC are available at https://quotsoft.net/air/ (last access: September 2024). AOD from MODIS Deep Blue retrieval are

available at https://modis.gsfc.nasa.gov/ (last access: September 2024). ERA5 reanalysis data are available at https://cds.climate.copernicus.eu/ (last access: September 2024). ~~CERES EBAF data are available at https://ceres.larc.nasa.gov/data/#energy-balanced-and-filled-ebaf (last access: September 2024).~~ GPM data are available at https://disc.gsfc.nasa.gov/datasets/GPM_3IMERGM_07/summary?keywords=%22IMERG%20final%22 (last access: September 2024). GPCP data are available at https://psl.noaa.gov/data/gridded/data.gpcp.html (last access: April 2025). The source code of CESM is available at https://github.com/ESCOMP/CESM (last access: September 2024). Our model results can be available at https://doi.org/10.5281/zenodo.13682943 (last access: September 2024).

Author Contributions

Y.Y. conceived the research and directed the analysis. J.G. conceived the research, conducted the model simulations, and performed the analysis. All the authors including H.W., P.W., and H. L. discussed the results and wrote the paper.

Competing Interests

At least one of the (co-)authors is a member of the editorial board of Atmospheric Chemistry and Physics. The peer-review process was guided by an independent editor, and the authors also have no other competing interests to declare.

References

Adler, R., Sapiano, M., Huffman, G., Wang, J.-J., Gu, G., Bolvin, D., Chiu, L., Schneider, U., Becker, A., Nelkin, E., Xie, P., Ferraro, R., and Shin, D.-B.: The Global Precipitation Climatology Project (GPCP) Monthly Analysis (New Version 2.3) and a Review of 2017 Global Precipitation, Atmosphere, 9, 138, https://doi.org/10.3390/atmos9040138, 2018.

Basha, G., Kishore, P., Venkat Ratnam, M., Ouarda, T. B. M. J., Velicogna, I., and Sutterley, T.: Vertical and latitudinal variation of the intertropical convergence zone derived using GPS radio occultation measurements, Remote Sens. Environ., 163, 262–269, https://doi.org/10.1016/j.rse.2015.03.024, 2015.

Beck, J. W., Zhou, W., Li, C., Wu, Z., White, L., Xian, F., Kong, X., and An, Z.: A 550,000-year record of East Asian monsoon rainfall from 10Be in loess, Science, 360, 877–881, https://doi.org/10.1126/science.aam5825, 2018.

Boer, M. M., Resco De Dios, V., and Bradstock, R. A.: Unprecedented burn area of Australian mega forest fires, Nat. Clim. Change, 10, 171–172, https://doi.org/10.1038/s41558-020-0716-1, 2020.

Bollasina, M. A., Ming, Y., and Ramaswamy, V.: Anthropogenic Aerosols and the Weakening of the South Asian Summer Monsoon, Science, 334, 502–505, https://doi.org/10.1126/science.1204994, 2011.

Bollasina, M. A., Ming, Y., Ramaswamy, V., Schwarzkopf, M. D., and Naik, V.: Contribution of local and remote anthropogenic aerosols to the twentieth century weakening of the South Asian Monsoon, Geophys. Res. Lett., 41, 680–687, https://doi.org/10.1002/2013GL058183, 2014.

Chiang, F., Mazdiyasni, O., and AghaKouchak, A.: Amplified warming of droughts in southern United States in observations and model simulations, Sci. Adv., 4, eaat2380, https://doi.org/10.1126/sciadv.aat2380, 2018.

Chiang, J. C. H., Fung, I. Y., Wu, C.-H., Cai, Y., Edman, J. P., Liu, Y., Day, J. A., Bhattacharya, T., Mondal, Y., and Labrousse, C. A.: Role of seasonal transitions and westerly jets in East Asian paleoclimate, Quat. Sci. Rev., 108, 111–129, https://doi.org/10.1016/j.quascirev.2014.11.009, 2015.

Collins, L., Clarke, H., Clarke, M. F., McColl Gausden, S. C., Nolan, R. H., Penman, T., and Bradstock, R.: Warmer and drier conditions have increased the potential for large and severe fire seasons across south-eastern Australia, Glob. Ecol. Biogeogr., 31, 1933–1948, https://doi.org/10.1111/geb.13514, 2022.

Cook, B. I. and Seager, R.: The response of the North American Monsoon to increased greenhouse gas forcing, J. Geophys. Res.: Atmos., 118, 1690–1699, https://doi.org/10.1002/jgrd.50111, 2013.

Cowan, T. and Cai, W.: The impact of Asian and non-Asian anthropogenic aerosols on 20th century Asian summer monsoon: ASIAN MONSOON AND AEROSOLS, Geophys. Res. Lett., 38, L11703, https://doi.org/10.1029/2011GL047268, 2011.

CSIRO and BOM: State of the Climate 2022, 2022

Dang, R. and Liao, H.: Radiative Forcing and Health Impact of Aerosols and Ozone in China as the Consequence of Clean Air Actions over 2012–2017, Geophys. Res. Lett., 46, 12511–12519, https://doi.org/10.1029/2019GL084605, 2019.

Dey, R., Lewis, S. C., Arblaster, J. M., and Abram, N. J.: A review of past and projected changes in Australia's rainfall, WIREs Clim. Change, 10, e577, https://doi.org/10.1002/wcc.577, 2019a.

Dey, R., Lewis, S. C., and Abram, N. J.: Investigating observed northwest Australian rainfall trends in Coupled Model Intercomparison Project phase 5 detection and attribution experiments, Int. J. Climatol., 39, 112–127, https://doi.org/10.1002/joc.5788, 2019b.

Dong, B., Wilcox, L. J., Highwood, E. J., and Sutton, R. T.: Impacts of recent decadal changes in Asian aerosols on the East Asian summer monsoon: roles of aerosol–radiation and aerosol–cloud interactions, Clim. Dyn., 53, 3235–3256, https://doi.org/10.1007/s00382-019-04698-0, 2019.

Dowdy, A. J.: Seamless climate change projections and seasonal predictions for bushfires in Australia, J. South. Hemisph. Earth Syst. Sci., 70, 120–138, https://doi.org/10.1071/ES20001, 2020.

Evans, S., Marchand, R., and Ackerman, T.: Variability of the Australian Monsoon and Precipitation Trends at Darwin, J. Climate, 27, 8487–8500, https://doi.org/10.1175/JCLI-D-13-00422.1, 2014.

Fahrenbach, N. L. S., Bollasina, M. A., Samset, B. H., Cowan, T., and Ekman, A. M. L.: Asian anthropogenic aerosol forcing played a key role in the multi-decadal increase in Australian summer monsoon rainfall, J. Climate, 1, https://doi.org/10.1175/JCLI-D-23-0313.1, 2023.

Fan, T., Liu, X., Ma, P.-L., Zhang, Q., Li, Z., Jiang, Y., Zhang, F., Zhao, C., Yang, X., Wu, F., and Wang, Y.: Emission or atmospheric processes? An attempt to attribute the source of large bias of aerosols in eastern China simulated by global climate models, Atmos. Chem. Phys., 18, 1395–1417, https://doi.org/10.5194/acp-18-1395-2018, 2018.

Fan, T., Liu, X., Wu, C., Zhang, Q., Zhao, C., Yang, X., and Li, Y.: Comparison of the Anthropogenic Emission Inventory for CMIP6 Models with a Country-Level Inventory over China and the Simulations of the Aerosol Properties, Adv. Atmos. Sci., 39, 80–96, https://doi.org/10.1007/s00376-021-1119-6, 2022.

Fischer, E. M., Seneviratne, S. I., Lüthi, D., and Schär, C.: Contribution of land-atmosphere coupling to recent European summer heat waves, Geophys. Res. Lett., 34, 2006GL029068, https://doi.org/10.1029/2006GL029068, 2007.

Gao, J., Yang, Y., Wang, H., Wang, P., Li, H., Li, M., Ren, L., Yue, X., and Liao, H.: Fast climate responses to emission reductions in aerosol and ozone precursors in China during 2013–2017, Atmos. Chem. Phys., 22, 7131–7142, https://doi.org/10.5194/acp-22-7131-2022, 2022.

Gao, J., Yang, Y., Wang, H., Wang, P., Li, B., Li, J., Wei, J., Gao, M., and Liao, H.: Climate responses in China to domestic and foreign aerosol changes due to clean air actions during 2013–2019, npj Clim. Atmos. Sci., 6, 160, https://doi.org/10.1038/s41612-023-00488-y, 2023.

Giani, P., Castruccio, S., Anav, A., Howard, D., Hu, W., and Crippa, P.: Short-term and long-term health impacts of air pollution reductions from COVID-19 lockdowns in China and Europe: a modelling study, Lancet Planet. Health, 4, e474–e482, https://doi.org/10.1016/S2542-5196(20)30224-2, 2020.

Guenther, A. B., Jiang, X., Heald, C. L., Sakulyanontvittaya, T., Duhl, T., Emmons, L. K., and Wang, X.: The Model of Emissions of Gases and Aerosols from Nature version 2.1

(MEGAN2.1): an extended and updated framework for modeling biogenic emissions, Geosci. Model Dev., 5, 1471–1492, https://doi.org/10.5194/gmd-5-1471-2012, 2012.

He, T., Lamont, B. B., and Pausas, J. G.: Fire as a key driver of Earth's biodiversity, Biol. Rev., 94, 1983–2010, https://doi.org/10.1111/brv.12544, 2019.

Head, L., Adams, M., McGregor, H. V., and Toole, S.: Climate change and Australia, WIREs Clim. Change, 5, 175–197, https://doi.org/10.1002/wcc.255, 2014.

Heidemann, H., Cowan, T., Henley, B. J., Ribbe, J., Freund, M., and Power, S.: Variability and long-term change in Australian monsoon rainfall: A review, WIREs Clim. Change, 14, e823, https://doi.org/10.1002/wcc.823, 2023.

Hersbach, H., Bell, B., Berrisford, P., Hirahara, S., Horányi, A., Muñoz-Sabater, J., Nicolas, J., Peubey, C., Radu, R., Schepers, D., Simmons, A., Soci, C., Abdalla, S., Abellan, X., Balsamo, G., Bechtold, P., Biavati, G., Bidlot, J., Bonavita, M., De Chiara, G., Dahlgren, P., Dee, D., Diamantakis, M., Dragani, R., Flemming, J., Forbes, R., Fuentes, M., Geer, A., Haimberger, L., Healy, S., Hogan, R. J., Hólm, E., Janisková, M., Keeley, S., Laloyaux, P., Lopez, P., Lupu, C., Radnoti, G., De Rosnay, P., Rozum, I., Vamborg, F., Villaume, S., and Thépaut, J.: The ERA5 global reanalysis, Q. J. R. Meteorol. Soc., 146, 1999–2049, https://doi.org/10.1002/qj.3803, 2020.

Hoesly, R. M., Smith, S. J., Feng, L., Klimont, Z., Janssens-Maenhout, G., Pitkanen, T., Seibert, J. J., Vu, L., Andres, R. J., Bolt, R. M., Bond, T. C., Dawidowski, L., Kholod, N., Kurokawa, J., Li, M., Liu, L., Lu, Z., Moura, M. C. P., O'Rourke, P. R., and Zhang, Q.: Historical (1750–2014) anthropogenic emissions of reactive gases and aerosols from the Community Emissions Data System (CEDS), Geosci. Model Dev., 11, 369–408, https://doi.org/10.5194/gmd-11-369-2018, 2018.

Hsu, N. C., Jeong, M. -J., Bettenhausen, C., Sayer, A. M., Hansell, R., Seftor, C. S., Huang, J., and Tsay, S. -C.: Enhanced Deep Blue aerosol retrieval algorithm: The second generation, J. Geophys. Res.: Atmos., 118, 9296–9315, https://doi.org/10.1002/jgrd.50712, 2013.

Huneeus, N., Denier Van Der Gon, H., Castesana, P., Menares, C., Granier, C., Granier, L., Alonso, M., De Fatima Andrade, M., Dawidowski, L., Gallardo, L., Gomez, D., Klimont, Z., Janssens-Maenhout, G., Osses, M., Puliafito, S. E., Rojas, N., Ccoyllo, O. S.-, Tolvett, S., and Ynoue, R. Y.: Evaluation of anthropogenic air pollutant emission inventories for South America at national and city scale, Atmos. Environ., 235, 117606, https://doi.org/10.1016/j.atmosenv.2020.117606, 2020.

IPCC: Climate Change 2013: The Physical Science Basis, 2013.

IPCC: Climate Change 2021: The Physical Science Basis, 2021.

Irmak, S., Irmak, A., Allen, R. G., and Jones, J. W.: Solar and Net Radiation-Based Equations to Estimate Reference Evapotranspiration in Humid Climates, J. Irrig. Drain. Eng., 129, 336–347, https://doi.org/10.1061/(ASCE)0733-9437(2003)129:5(336), 2003.

Johnston, F. H., Borchers-Arriagada, N., Morgan, G. G., Jalaludin, B., Palmer, A. J., Williamson, G. J., and Bowman, D. M. J. S.: Unprecedented health costs of smoke-related PM2.5 from the 2019–20 Australian megafires, Nat. Sustain., 4, 42–47, https://doi.org/10.1038/s41893-020-00610-5, 2021.

Jones, M. W., Abatzoglou, J. T., Veraverbeke, S., Andela, N., Lasslop, G., Forkel, M., Smith, A. J. P., Burton, C., Betts, R. A., van der Werf, G. R., Sitch, S., Canadell, J. G., Santín, C., Kolden, C., Doerr, S. H., and Le Quéré, C.: Global and Regional Trends and Drivers of Fire Under Climate Change, Rev. Geophys., 60, e2020RG000726, https://doi.org/10.1029/2020RG000726, 2022.

Kloster, S., Dentener, F., Feichter, J., Raes, F., Lohmann, U., Roeckner, E., and Fischer-Bruns, I.: A GCM study of future climate response to aerosol pollution reductions, Clim. Dyn., 34, 1177–1194, https://doi.org/10.1007/s00382-009-0573-0, 2010.

Lau, K.-M. and Kim, K.-M.: Observational relationships between aerosol and Asian monsoon rainfall, and circulation, Geophys. Res. Lett., 33, 2006GL027546, https://doi.org/10.1029/2006GL027546, 2006.

Leibensperger, E. M., Mickley, L. J., Jacob, D. J., Chen, W.-T., Seinfeld, J. H., Nenes, A., Adams, P. J., Streets, D. G., Kumar, N., and Rind, D.: Climatic effects of 1950–2050 changes in US anthropogenic aerosols – Part 1: Aerosol trends and radiative forcing, Atmos. Chem. Phys., 12, 3333–3348, https://doi.org/10.5194/acp-12-3333-2012, 2012.

Liu, C., Yang, Y., Wang, H., Ren, L., Wei, J., Wang, P., and Liao, H.: Influence of Spatial Dipole Pattern in Asian Aerosol Changes on East Asian Summer Monsoon, J. Climate, 36, 1575–1585, https://doi.org/10.1175/JCLI-D-22-0335.1, 2023.

Liu, X., Ma, P.-L., Wang, H., Tilmes, S., Singh, B., Easter, R. C., Ghan, S. J., and Rasch, P. J.: Description and evaluation of a new four-mode version of the Modal Aerosol Module (MAM4) within version 5.3 of the Community Atmosphere Model, Geosci. Model Dev., 9, 505–522, https://doi.org/10.5194/gmd-9-505-2016, 2016.

~~Loeb, N. G., Doelling, D. R., Wang, H., Su, W., Nguyen, C., Corbett, J. G., Liang, L., Mitrescu, C., Rose, F. G., and Kato, S.: Clouds and the Earth's Radiant Energy System (CERES) Energy Balanced and Filled (EBAF) Top-of-Atmosphere (TOA) Edition-4.0 Data Product, J. Climate, 31, 895–918, https://doi.org/10.1175/JCLI-D-17-0208.1, 2018.~~

Ming, Y. and Ramaswamy, V.: Nonlinear Climate and Hydrological Responses to Aerosol Effects, J. Climate, 22, 1329–1339, https://doi.org/10.1175/2008JCLI2362.1, 2009.

Moritz, M. A., Batllori, E., Bradstock, R. A., Gill, A. M., Handmer, J., Hessburg, P. F., Leonard, J., McCaffrey, S., Odion, D. C., Schoennagel, T., and Syphard, A. D.: Learning to coexist with wildfire, Nature, 515, 58–66, https://doi.org/10.1038/nature13946, 2014.

Nicholls, N.: Detecting and attributing Australian climate change: a review, Aust. Meteorol. Mag., 2006.

Oh, H. and Ha, K.-J.: Thermodynamic characteristics and responses to ENSO of dominant intraseasonal modes in the East Asian summer monsoon, Clim. Dyn., 44, 1751–1766, https://doi.org/10.1007/s00382-014-2268-4, 2015.

Pozzoli, L., Janssens-Maenhout, G., Diehl, T., Bey, I., Schultz, M. G., Feichter, J., Vignati, E., and Dentener, F.: Re-analysis of tropospheric sulfate aerosol and ozone for the period 1980–2005 using the aerosol-chemistry-climate model ECHAM5-HAMMOZ, Atmos. Chem. Phys., 11, 9563–9594, https://doi.org/10.5194/acp-11-9563-2011, 2011.

Rauniyar, S. P. and Power, S. B.: The Impact of Anthropogenic Forcing and Natural Processes on Past, Present, and Future Rainfall over Victoria, Australia, J. Climate, 33, 8087–8106, https://doi.org/10.1175/JCLI-D-19-0759.1, 2020.

Ren, L., Yang, Y., Wang, H., Wang, P., Yue, X., and Liao, H.: Widespread Wildfires Over the Western United States in 2020 Linked to Emissions Reductions During COVID-19, Geophys. Res. Lett., 49, e2022GL099308, https://doi.org/10.1029/2022GL099308, 2022.

Risbey, J. S., Pook, M. J., McIntosh, P. C., Wheeler, M. C., and Hendon, H. H.: On the Remote Drivers of Rainfall Variability in Australia, Mon. Wea. Rev., 137, 3233–3253, https://doi.org/10.1175/2009MWR2861.1, 2009.

Rotstayn, L. D., Cai, W., Dix, M. R., Farquhar, G. D., Feng, Y., Ginoux, P., Herzog, M., Ito, A., Penner, J. E., Roderick, M. L., and Wang, M.: Have Australian rainfall and cloudiness increased due to the remote effects of Asian anthropogenic aerosols?, J. Geophys. Res.: Atmos., 112, 2006JD007712, https://doi.org/10.1029/2006JD007712, 2007.

Samset, B. H., Lund, M. T., Bollasina, M., Myhre, G., and Wilcox, L.: Emerging Asian aerosol patterns, Nat. Geosci., 12, 582–584, https://doi.org/10.1038/s41561-019-0424-5, 2019.

Schiemann, R., Lüthi, D., and Schär, C.: Seasonality and Interannual Variability of the Westerly Jet in the Tibetan Plateau Region, J. Climate, 22, 2940–2957, https://doi.org/10.1175/2008JCLI2625.1, 2009.

Seager, R., Hooks, A., Williams, A. P., Cook, B., Nakamura, J., and Henderson, N.: Climatology, Variability, and Trends in the U.S. Vapor Pressure Deficit, an Important Fire-Related Meteorological Quantity, J. Appl. Meteorol. Clim., 54, 1121–1141, https://doi.org/10.1175/JAMC-D-14-0321.1, 2015.

Seneviratne, S. I., Lüthi, D., Litschi, M., and Schär, C.: Land–atmosphere coupling and climate change in Europe, Nature, 443, 205–209, https://doi.org/10.1038/nature05095, 2006.

Sharples, J. J., McRae, R. H. D., Weber, R. O., and Gill, A. M.: A simple index for assessing fire danger rating, Environ. Modell. Softw., 24, 764–774, https://doi.org/10.1016/j.envsoft.2008.11.004, 2009.

Shi, G., Yan, H., Zhang, W., Dodson, J., Heijnis, H., and Burrows, M.: Rapid warming has resulted in more wildfires in northeastern Australia, Sci. Total Environ., 771, 144888, https://doi.org/10.1016/j.scitotenv.2020.144888, 2021.

Skofronick-Jackson, G., Petersen, W. A., Berg, W., Kidd, C., Stocker, E. F., Kirschbaum, D. B., Kakar, R., Braun, S. A., Huffman, G. J., Iguchi, T., Kirstetter, P. E., Kummerow, C., Meneghini, R., Oki, R., Olson, W. S., Takayabu, Y. N., Furukawa, K., and Wilheit, T.: The Global Precipitation Measurement (GPM) Mission for Science and Society, Bull. Am. Meteorol. Soc., 98, 1679–1695, https://doi.org/10.1175/BAMS-D-15-00306.1, 2017.

Streets, D. G., Yan, F., Chin, M., Diehl, T., Mahowald, N., Schultz, M., Wild, M., Wu, Y., and Yu, C.: Anthropogenic and natural contributions to regional trends in aerosol optical depth, 1980–2006, J. Geophys. Res.: Atmos., 114, 2008JD011624, https://doi.org/10.1029/2008JD011624, 2009.

Su, H., Yang, Z., Dickinson, R. E., and Wei, J.: Spring soil moisture-precipitation feedback in the Southern Great Plains: How is it related to large-scale atmospheric conditions?, Geophys. Res. Lett., 41, 1283–1289, https://doi.org/10.1002/2013GL058931, 2014.

Turnock, S. T., Allen, R. J., Andrews, M., Bauer, S. E., Deushi, M., Emmons, L., Good, P., Horowitz, L., John, J. G., Michou, M., Nabat, P., Naik, V., Neubauer, D., O'Connor, F. M., Olivié, D., Oshima, N., Schulz, M., Sellar, A., Shim, S., Takemura, T., Tilmes, S., Tsigaridis, K., Wu, T., and Zhang, J.: Historical and future changes in air pollutants from CMIP6 models, Atmos. Chem. Phys., 20, 14547–14579, https://doi.org/10.5194/acp-20-14547-2020, 2020.

Undorf, S., Polson, D., Bollasina, M. A., Ming, Y., Schurer, A., and Hegerl, G. C.: Detectable Impact of Local and Remote Anthropogenic Aerosols on the 20th Century Changes of West African and South Asian Monsoon Precipitation, J. Geophys. Res.: Atmos., 123, 4871–4889, https://doi.org/10.1029/2017JD027711, 2018.

Van Marle, M. J. E., Kloster, S., Magi, B. I., Marlon, J. R., Daniau, A.-L., Field, R. D., Arneth, A., Forrest, M., Hantson, S., Kehrwald, N. M., Knorr, W., Lasslop, G., Li, F., Mangeon, S., Yue, C., Kaiser, J. W., and Van Der Werf, G. R.: Historic global biomass burning emissions for CMIP6 (BB4CMIP) based on merging satellite observations with proxies and fire models (1750–2015), Geosci. Model Dev., 10, 3329–3357, https://doi.org/10.5194/gmd-10-3329-2017, 2017.

Wang, B., Biasutti, M., Byrne, M. P., Castro, C., Chang, C.-P., Cook, K., Fu, R., Grimm, A. M., Ha, K.-J., Hendon, H., Kitoh, A., Krishnan, R., Lee, J.-Y., Li, J., Liu, J., Moise, A., Pascale, S., Roxy, M. K., Seth, A., Sui, C.-H., Turner, A., Yang, S., Yun, K.-S., Zhang, L., and Zhou, T.: Monsoons Climate Change Assessment, Bull. Am. Meteorol. Soc., 102, E1–E19, https://doi.org/10.1175/BAMS-D-19-0335.1, 2021.

Wang, H., Easter, R. C., Rasch, P. J., Wang, M., Liu, X., Ghan, S. J., Qian, Y., Yoon, J.-H., Ma, P.-L., and Vinoj, V.: Sensitivity of remote aerosol distributions to representation of cloud–aerosol interactions in a global climate model, Geosci. Model Dev., 6, 765–782, https://doi.org/10.5194/gmd-6-765-2013, 2013.

Wang, P., Yang, Y., Xue, D., Ren, L., Tang, J., Leung, L. R., and Liao, H.: Aerosols overtake greenhouse gases causing a warmer climate and more weather extremes toward carbon neutrality, Nat. Commun., 14, 7257, https://doi.org/10.1038/s41467-023-42891-2, 2023.

Wang, Z., Zhang, H., and Zhang, X.: Projected response of East Asian summer monsoon system to future reductions in emissions of anthropogenic aerosols and their precursors, Clim. Dyn., 47, 1455–1468, https://doi.org/10.1007/s00382-015-2912-7, 2016.

Wang, Z., Lin, L., Xu, Y., Che, H., Zhang, X., Zhang, H., Dong, W., Wang, C., Gui, K., and Xie, B.: Incorrect Asian aerosols affecting the attribution and projection of regional climate change in CMIP6 models, npj Clim. Atmos. Sci., 4, 2, https://doi.org/10.1038/s41612-020-00159-2, 2021.

Ward, M., Tulloch, A. I. T., Radford, J. Q., Williams, B. A., Reside, A. E., Macdonald, S. L., Mayfield, H. J., Maron, M., Possingham, H. P., Vine, S. J., O'Connor, J. L., Massingham, E. J., Greenville, A. C., Woinarski, J. C. Z., Garnett, S. T., Lintermans, M., Scheele, B. C., Carwardine, J., Nimmo, D. G., Lindenmayer, D. B., Kooyman, R. M., Simmonds, J. S., Sonter, L. J., and Watson, J. E. M.: Impact of 2019–2020 mega-fires on Australian fauna habitat, Nat. Ecol. Evol., 4, 1321–1326, https://doi.org/10.1038/s41559-020-1251-1, 2020.

Wasko, C., Shao, Y., Vogel, E., Wilson, L., Wang, Q. J., Frost, A., and Donnelly, C.: Understanding trends in hydrologic extremes across Australia, J. Hydrol., 593, 125877, https://doi.org/10.1016/j.jhydrol.2020.125877, 2021.

Yang, Y., Zeng, L., Wang, H., Wang, P., and Liao, H.: Climate effects of future aerosol reductions for achieving carbon neutrality in China, Sci. Bull., 68, 902–905, https://doi.org/10.1016/j.scib.2023.03.048, 2023.

Zacharakis, I. and Tsihrintzis, V. A.: Integrated wildfire danger models and factors: A review, Sci. Total Environ., 899, 165704, https://doi.org/10.1016/j.scitotenv.2023.165704, 2023.

Zeng, L., Yang, Y., Wang, H., Wang, J., Li, J., Ren, L., Li, H., Zhou, Y., Wang, P., and Liao, H.: Intensified modulation of winter aerosol pollution in China by El Niño with short duration, Atmos. Chem. Phys., 21, 10745–10761, https://doi.org/10.5194/acp-21-10745-2021, 2021.

Zhang, Q., Zheng, Y., Tong, D., Shao, M., Wang, S., Zhang, Y., Xu, X., Wang, J., He, H., Liu, W., Ding, Y., Lei, Y., Li, J., Wang, Z., Zhang, X., Wang, Y., Cheng, J., Liu, Y., Shi, Q., Yan, L., Geng, G., Hong, C., Li, M., Liu, F., Zheng, B., Cao, J., Ding, A., Gao, J., Fu, Q., Huo, J., Liu, B., Liu, Z., Yang, F., He, K., and Hao, J.: Drivers of improved PM2.5 air quality in China from 2013 to 2017, Proc. Natl. Acad. Sci., 116, 24463–24469, https://doi.org/10.1073/pnas.1907956116, 2019.

Zheng, B., Tong, D., Li, M., Liu, F., Hong, C., Geng, G., Li, H., Li, X., Peng, L., Qi, J., Yan, L., Zhang, Y., Zhao, H., Zheng, Y., He, K., and Zhang, Q.: Trends in China's anthropogenic emissions since 2010 as the consequence of clean air actions, Atmos. Chem. Phys., 18, 14095–14111, https://doi.org/10.5194/acp-18-14095-2018, 2018.

Zheng, Y., Xue, T., Zhang, Q., Geng, G., Tong, D., Li, X., and He, K.: Air quality improvements and health benefits from China's clean air action since 2013, Environ. Res. Lett., 12, 114020, https://doi.org/10.1088/1748-9326/aa8a32, 2017.

1286   Zheng, Y., Zhang, Q., Tong, D., Davis, S. J., and Caldeira, K.: Climate effects of China's efforts
1287   to improve its air quality, Environ. Res. Lett., 15, 104052, https://doi.org/10.1088/1748-
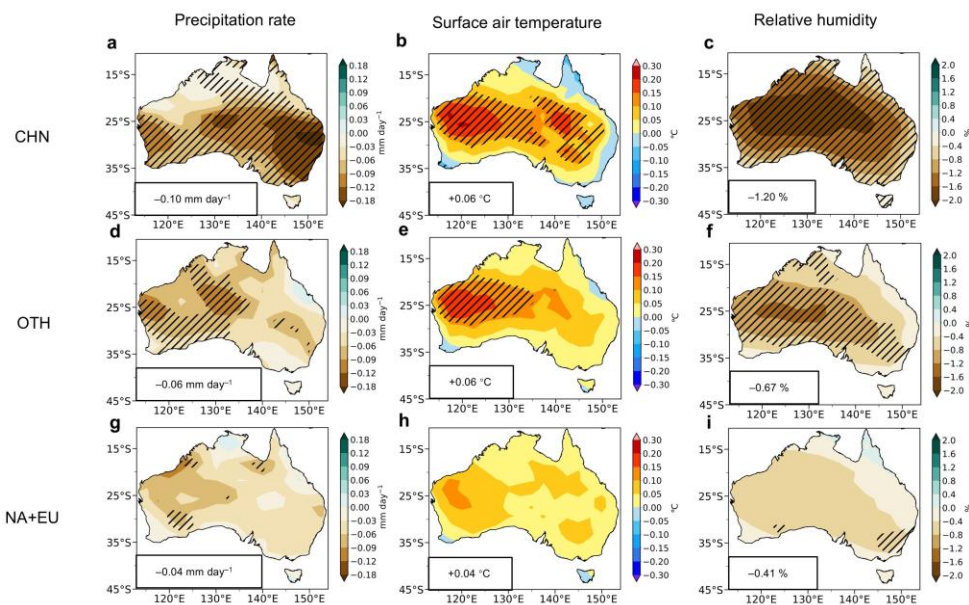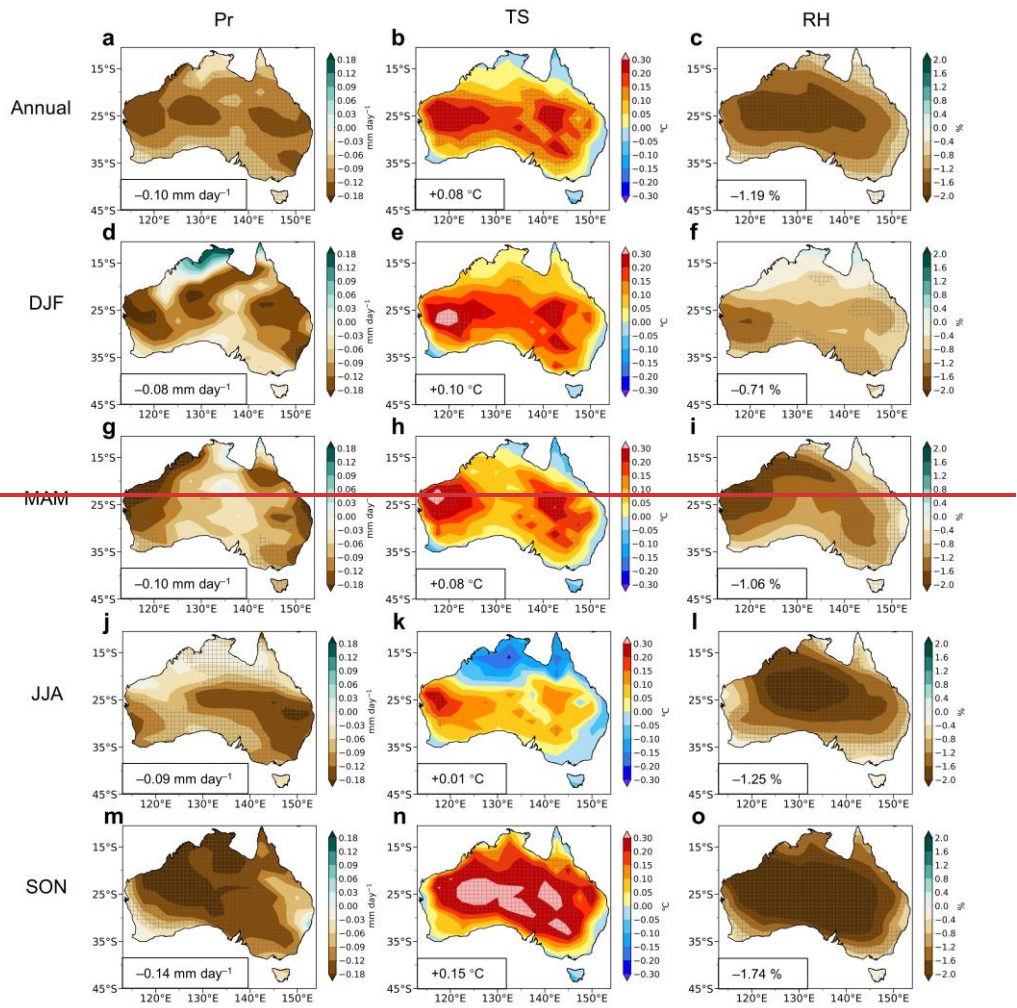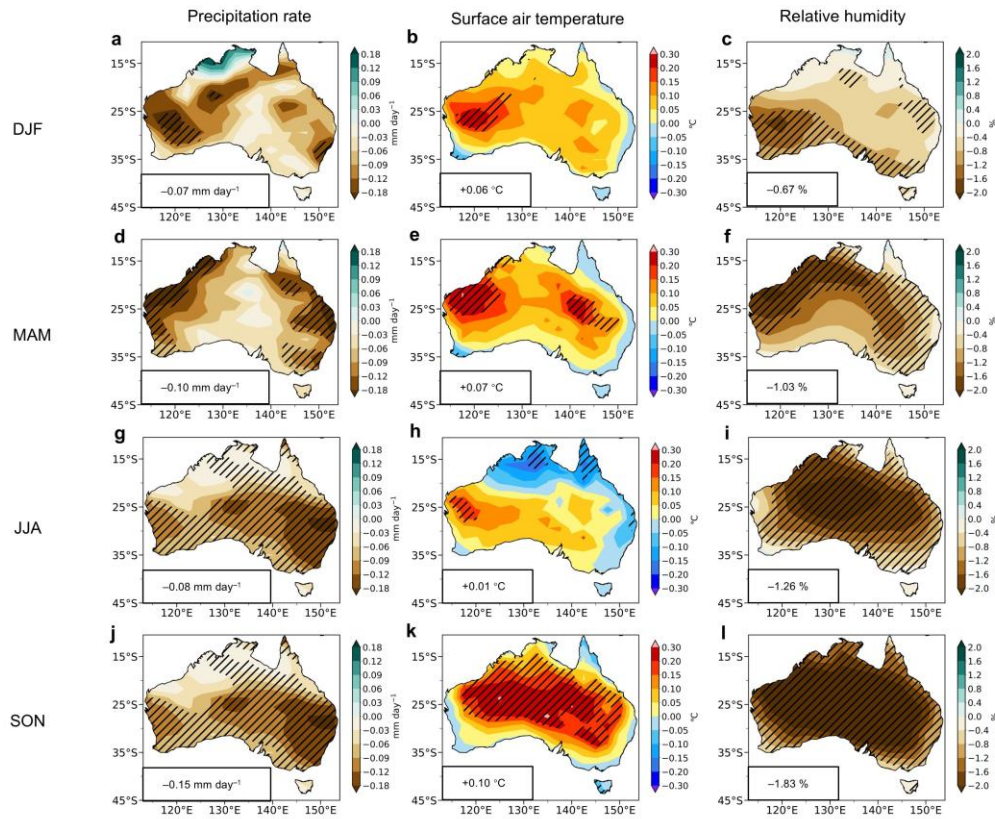1288   9326/ab9e21, 2020.
1289

Figure 1.

292 **Figure 1. Simulated changes in precipitation rate, surface air temperature and relative**
293 **humidity in Australia due to aerosol changes between 2013 and 2019.** Spatial distributions of
294 simulated differences in annual mean precipitation rate (Pr, **a**, **d**, and **g**, unit: mm day^{-1}), surface
295 air temperature (TS, **b**, **e**, and **h**, unit: °C) and relative humidity (RH, **c**, **f**, and **i**, unit: %) in
296 Australia between BASE and CHN (CHN minus BASE, **a**–**c**), between BASE and OTH (OTH
297 minus BASE, **d**–**f**), and between BASE and NAEU (NAEU minus BASE, **g**–**i**). The shaded areas
298 indicate results are statistically significant at the 90% confidence level. Regional averages over
299 Australia are noted at the bottom-left corner of each panel.

300

301 **Figure 2.** **Simulated changes in precipitation rate, surface air temperature and relative**
302 **humidity in Australia due to aerosol changes in China between 2013 and 2019.** Spatial
303 distributions of simulated differences in ~~annual (a–c),~~ DJF (~~d–f,~~December, January and
304 February, **a**–**c**), MAM (~~g–I,~~March, April and May, **d**–**f**), JJA (~~j–l,~~June, July and August, **g**–**i**)
305 and SON (~~m–o,~~September, October and November, **j**–**l**) mean precipitation rate (Pr, **a**, **d**, **g**, ~~j,~~
306 and ~~m~~**j**, unit: mm day^{-1}), surface air temperature (TS, **b**, **e**, **h**, ~~k,~~and ~~n~~**k**, unit: °C) and relative

48

1307   humidity (RH, **c**, **f**, **i**, ~~l,~~ and ~~o~~l, unit: %) in Australia between BASE and CHN (CHN minus

1308   BASE). ~~The~~ The shaded areas indicate results are statistically significant at the 90% confidence level.

1309   Regional averages over Australia are noted at the bottom-left corner of each panel.
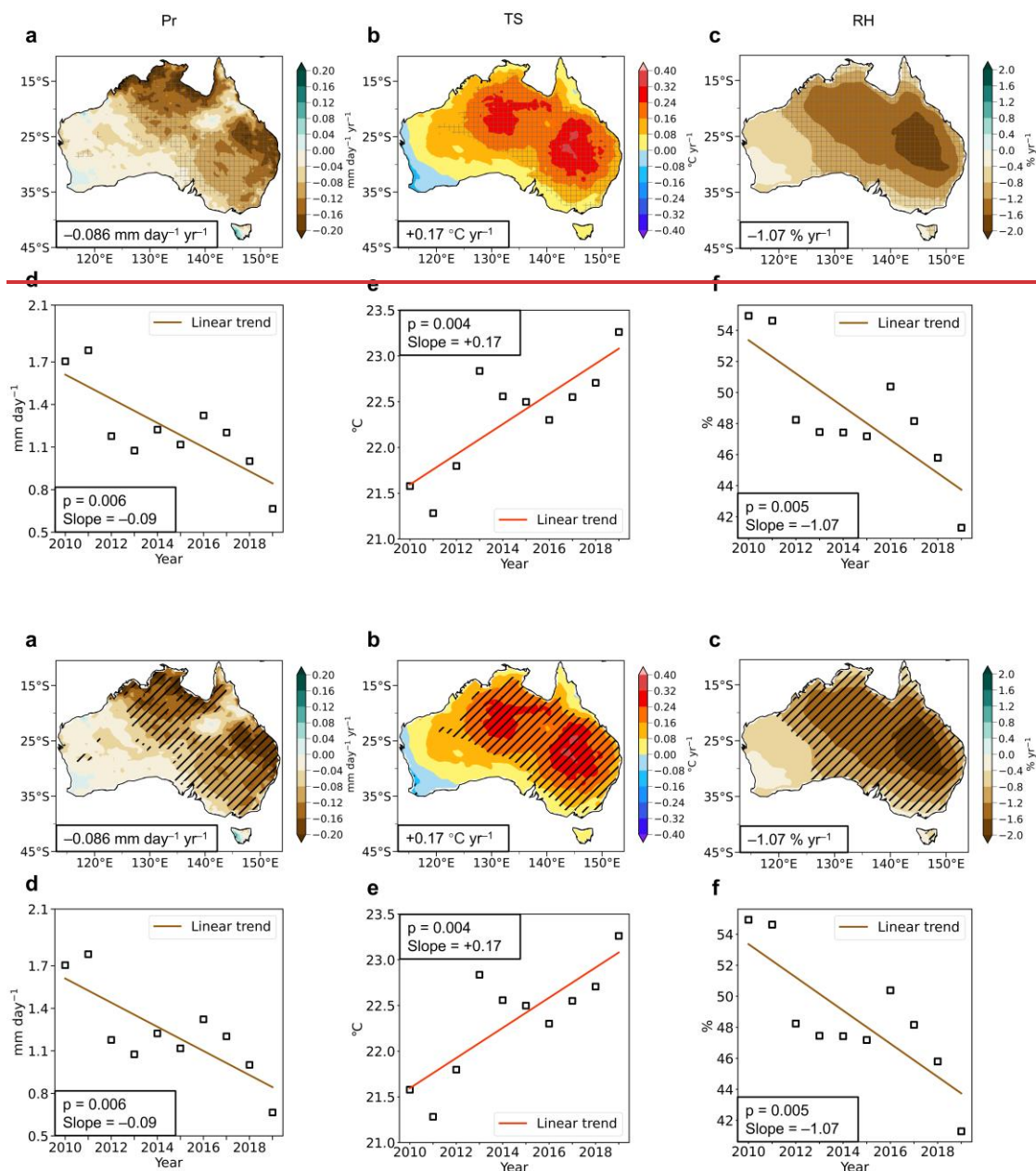
1310

Figure 23. **Linear trends of observed precipitation rate, surface air temperature and relative humidity in Australia based on ERA5.** Spatial distributions of linear trends (**a**, **b**, and **c**) and time series (**d**, **e**, and **f**) of annual mean precipitation rate (Pr, **a** and **d**, unit: mm day^{-1}), surface air temperature (TS, **b** and **e**, unit: °C) and relative humidity (RH, **c** and **f**, unit: %) in Australia during 2010–2019 from ERA5 reanalysis. The shaded areas indicate trends are statistically significant at

50

1318 the 90% confidence level. Regional averages over Australia are noted at the bottom-left corner of

1319 panels a, b, and c. The p values and slopes of linear trends are noted in panels d, e, and f.

1320

1321
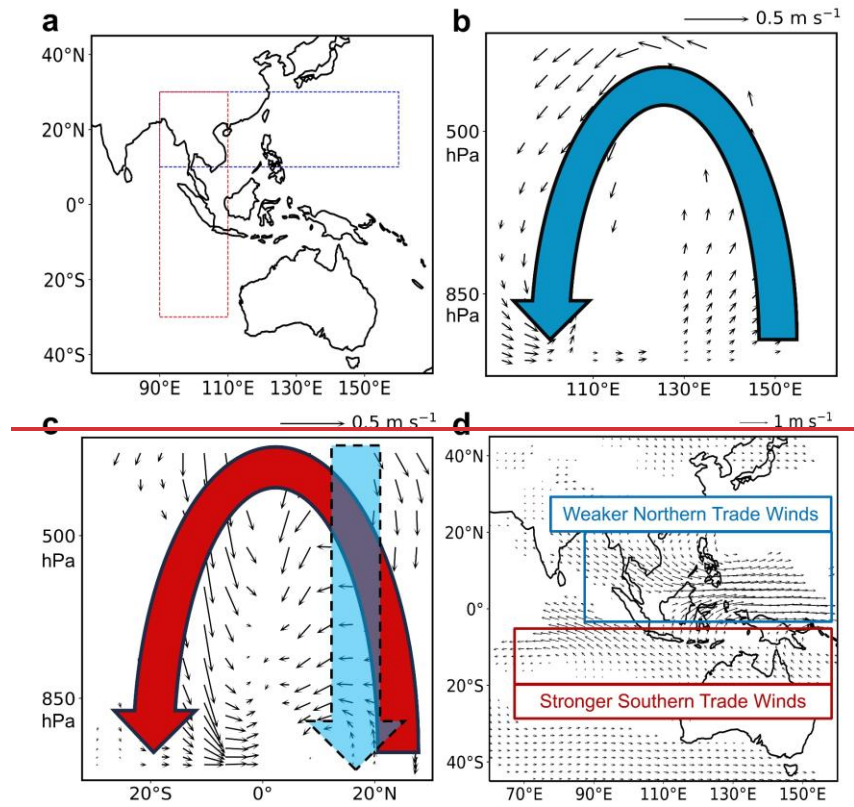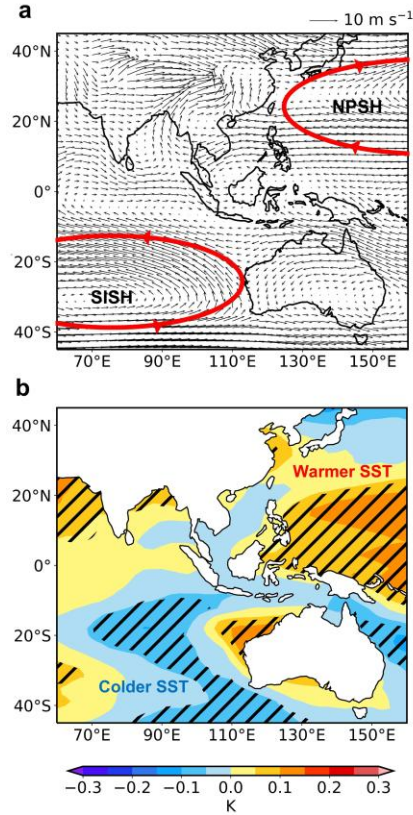
Figure 3.

Figure 4. Climatological mean wind fields at 850 hPa and Simulated sea surface temperature changes due to aerosol changes in China between 2013 and 2019. a, Climatological mean wind fields (unit: m s^{-1}, vectors) at 850 hPa from the BASE experiment. NPSH and SISH shown in red circles represents North Pacific Subtropical High and Southern Indian ocean Subtropical High, respectively. **b**, Spatial distributions of simulated differences in annual mean sea surface temperature (SST, unit: mm day^{-1}) in Australia between BASE and CHN (CHN minus BASE). The shaded areas indicate results are statistically significant at the 90% confidence level.
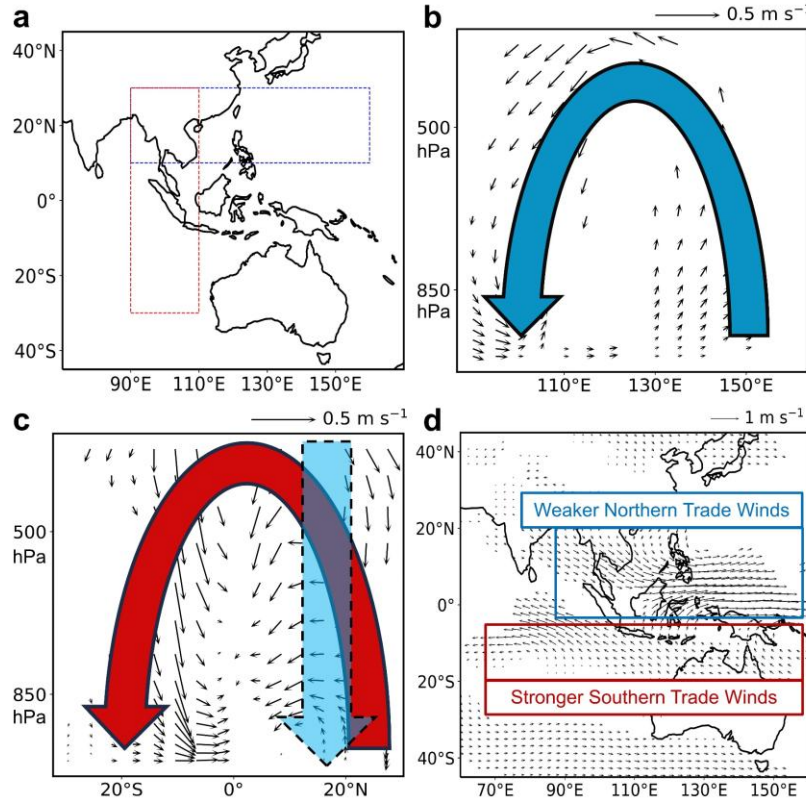
Figure 5. **Simulated changes in vertical circulations and 850 hPa wind fields in Asia-Pacific regions due to aerosol changes in China between 2013 and 2019.** Panel **b** and **c** shows pressure–longitude and pressure–latitude cross-section of responses in annual mean atmospheric circulations (unit: m s^{-1}, vectors), respectively, over the areas marked with the blue and red box in panel **a**. Panel **d** shows annual mean changes in wind fields (unit: m s^{-1}, vectors) at 850 hPa in Asia-Pacific regions. Only atmospheric circulations and winds statistically significant at the 90% confidence level are shown.
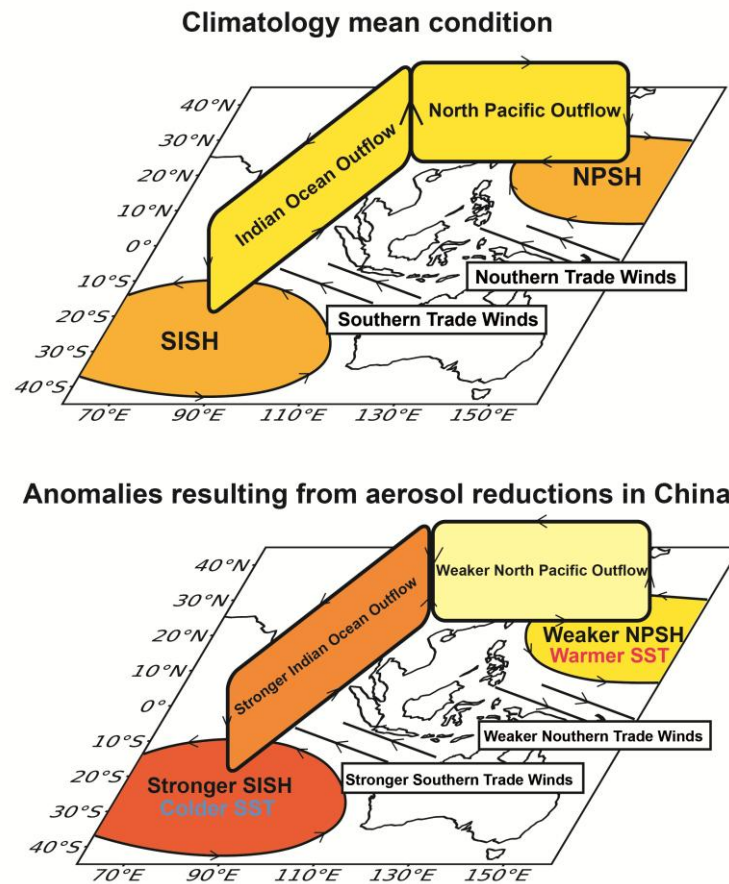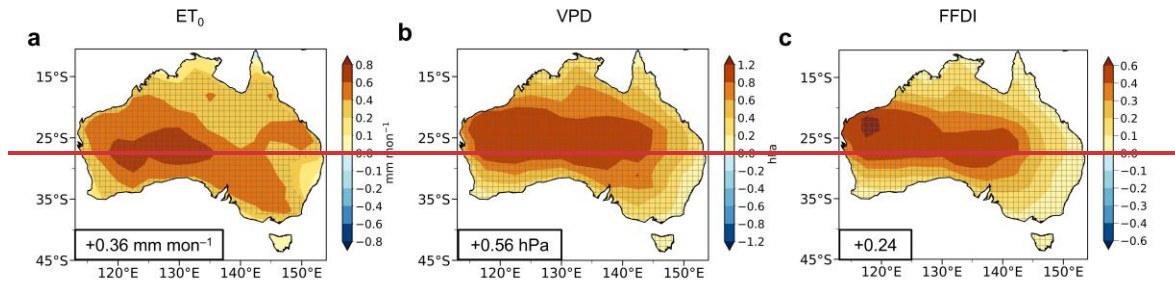
54

1341

1342   ~~Figure 4.~~ _____

1343   **Figure 6. Schematic of the response in large-scale 3D circulations in the Asian-Pacific**

1344   **region to aerosol reductions in China.** The top panel shows climatology mean condition, and

1345   the bottom panel shows anomalies resulting from aerosol reductions in China.
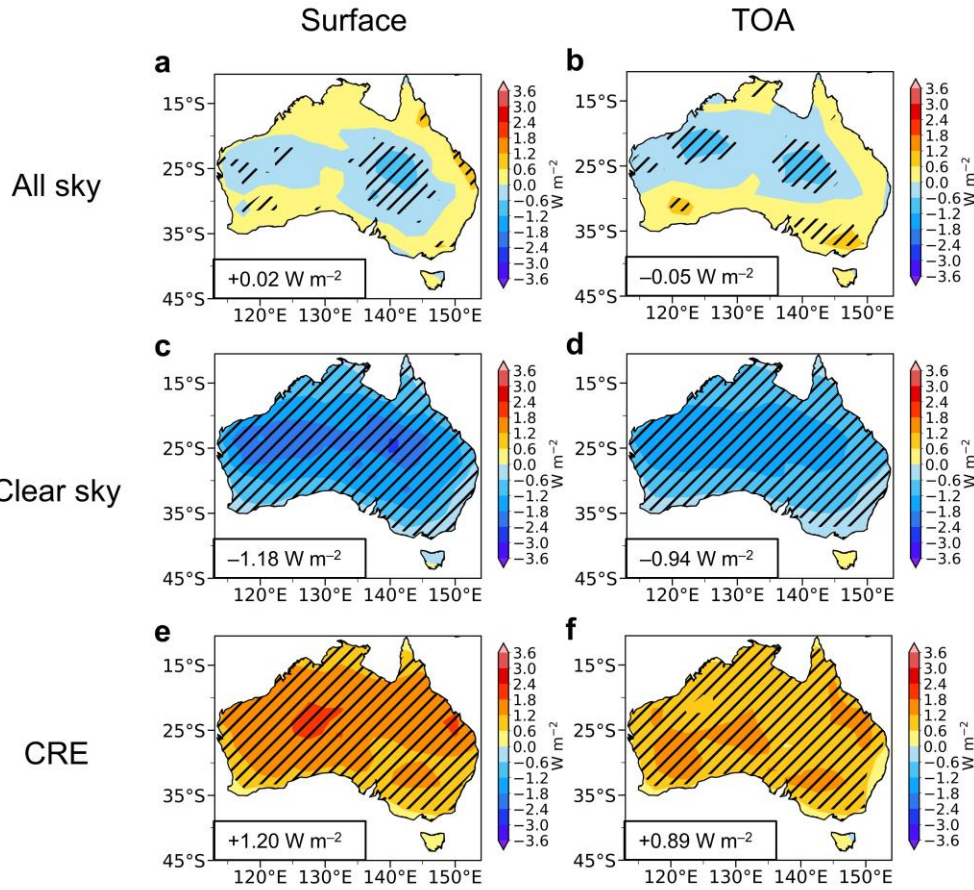
Figure 7. Simulated changes in surface and Top of the Atmosphere (TOA) net total radiative flux under all sky conditions, under clear sky conditions, and from cloud radiative effects in Australia due to aerosol changes in China between 2013 and 2019. Spatial distributions of simulated differences in annual mean surface (**a**, **c**, and **e**) and Top of the Atmosphere (TOA, **b**, **d**, and **f**) net total radiative flux (unit: W m^{-2}) under all sky conditions (**a** and **b**), under clear sky conditions (**c** and **d**), and from cloud radiative effects (CRE, **e** and **f**) in Australia between BASE and CHN (CHN minus BASE). Cloud radiative effects refer to differences under all sky and clear sky conditions (All sky minus Clear sky). The shaded areas indicate results are statistically significant at the 90% confidence level. Regional averages of the responses over Australia are noted at the bottom-left corner of each panel.
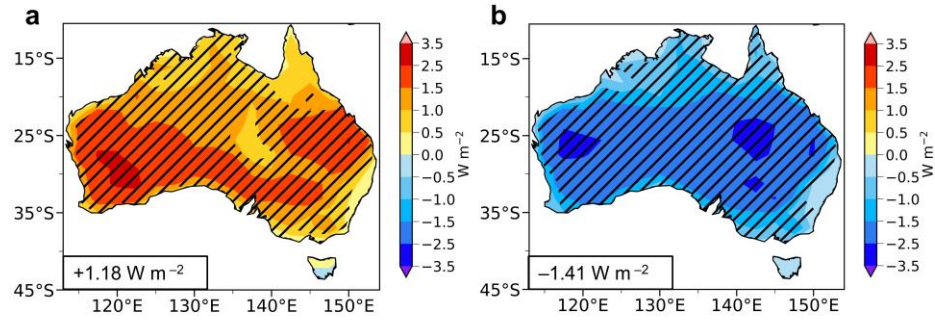
Figure 8. Simulated changes in surface upward sensible and latent heat flux in Australia due to aerosol changes in China between 2013 and 2019. Spatial distributions of simulated differences in annual mean surface upward sensible (**a**) and latent (**b**) heat flux (unit: W m^{-2}) in Australia between BASE and CHN (CHN minus BASE). The shaded areas indicate results are statistically significant at the 90% confidence level. Regional averages over Australia are noted at the bottom-left corner of each panel.
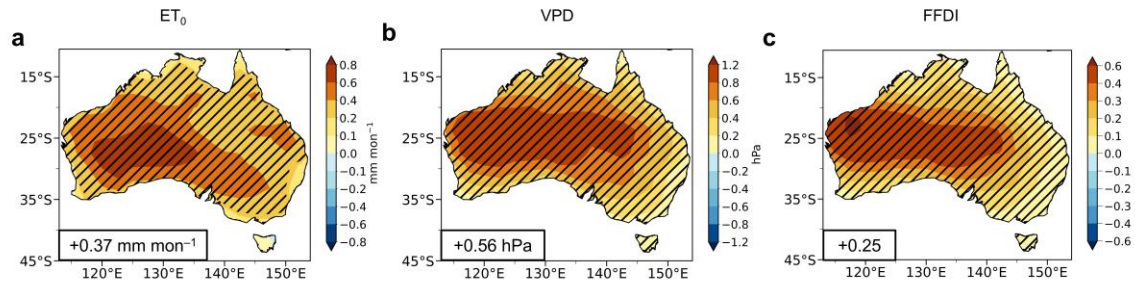
Figure 9. **Simulated changes in reference potential evapotranspiration, vapor pressure deficit, and McArthur forest fire danger index during fire seasons in Australia due to aerosol changes in China between 2013 and 2019.** Spatial distributions of simulated changes in reference potential evapotranspiration (ET$_0$, **a**, unit: mm mon^{-1}), vapor pressure deficit (VPD, **b**, unit: hPa), and McArthur forest fire danger index (FFDI, **c**, unitless) during fire seasons (austral spring and summer, from September to the February of the next year) in Australia between BASE and CHN (CHN minus BASE). The shaded areas indicate results are statistically significant at the 90% confidence level. Regional averages over Australia are noted at the bottom-left corner of each panel.

58